

**International
Progress Report**

IPR-03-39

Äspö Hard Rock Laboratory

Demonstration of deposition technology

Borehole radar measurements in D-tunnel, K-tunnel and TBM-hall

Seje Carlsten

GEOSIGMA AB Uppsala

June 1998

Svensk Kärnbränslehantering AB

Swedish Nuclear Fuel
and Waste Management Co
Box 5864
SE-102 40 Stockholm Sweden
Tel +46 8 459 84 00
Fax +46 8 661 57 19



**Äspö Hard Rock
Laboratory**

Report no.
IPR-03-39

Author
Seje Carlsten

Checked by

Approved
Christer Svemar

No.
F50K

Date
June 1998

Date

Date
2003-10-29

Äspö Hard Rock Laboratory

Demonstration of deposition technology

Borehole radar measurements in D-tunnel, K-tunnel and TBM-hall

Seje Carlsten

GEOSIGMA AB Uppsala

June 1998

Keywords: Borehole radar, high frequency antenna, reflector

This report concerns a study which was conducted for SKB. The conclusions and viewpoints presented in the report are those of the author(s) and do not necessarily coincide with those of the client.

Abstract

As part of the Demonstration of Deposition Technology Project at the Äspö HRL, borehole radar measurements with high frequency antenna using the RAMAC/GPR system were performed in totally 9 pilot-boreholes located in D-tunnel, K-tunnel, and in the TBM-hall. All boreholes were drilled vertically downwards from the floor at the respective tunnel section.

Most reflectors from the radar measurements exhibit a medium strong or weak magnitude in the radar maps. This is due to a combination of high salinity of groundwater and the large diameter (76 mm) of the investigated boreholes. The high resolution of the 250 MHz radar maps makes it possible to detect single fractures intersecting the boreholes.

High frequency radar reflectors have been correlated with mapped geological structures presented in core logs and with structures mapped and oriented with BIPS. The result of the correlation is considered good. The strike values are related to local Äspö north.

Sammanfattning

Som en del ingående i Demonstration of Deposition Technology Project har borrhålsradarmätningar med högfrequensantenn utförts i sammanlagt 9 borrhål ansatta i sulan i tunneln vid D-tunneln, K-tunneln och i TBM-hallen. Mätningarna utfördes med RAMAC/GPR systemet. Samtliga borrhål är vertikalt borrade.

De flesta reflektorer uppvisar en medelstark eller svag magnitud i radarbilderna. Detta beror på en kombination av hög salinitet på grundvattnet och den relativt stora borrhålsdiametern (76 mm) i de undersökta borrhålen. Den höga upplösningen hos 250 MHz radarbilderna har möjliggjort identifikation av enskilda sprickor vilka skär borrhålet.

Högfrequens reflektorerna har korrelerats med geologiska strukturer från kärnkartering och med strukturer vilka har karterats och orienterats med BIPS. Resultatet av korreleringen bedöms som god. Angivna riktningar i föreliggande rapport är relaterade till norr i det lokala Äspö koordinatsystemet.

Contents

Abstract	3
Sammanfattning	5
Contents	7
List of Figures	9
List of Tables	9
1 Introduction	11
2 Objectives	15
3 Equipment used	17
4 Data acquisition	19
5 Data processing	21
6 Results	23
6.1 General	23
6.2 High frequency antenna in the boreholes	24
6.2.1 Results from measurement in KA3147G01	25
6.2.2 Results from measurement in KA3153G01	26
6.2.3 Results from measurement in KK0025G01	27
6.2.4 Results from measurement in KK0031G01	29
6.2.5 Results from measurement in KK0037G01	30
6.2.6 Results from measurement in KK0045G01	32
6.2.7 Results from measurement in KK0051G01	34
6.2.8 Results from measurement in KD0086G01	36
6.2.9 Results from measurement in KD0092G01	38
7 Conclusions	41
References	43
Appendix: Bandpass filtered radar maps, moving-average filtered radar maps, and interpretation maps from the 250 MHz measurements.	45

List of Figures

Figure 1-1	Location of radar measured boreholes.	12
Figure 1-2	Location of radar measured borehole. Looking towards Äspö local north.	13
Figure 3-1	Equipment configuration used for the high frequency radar measurement in the boreholes.	18

List of Tables

Table 1-1	Borehole data for the radar investigated boreholes included in the Demonstration of Deposition Technology Project. All values are given in the Äspö local system and in relation to Äspö local north. Data has been provided by SKB.	11
Table 4-1	Specification of borehole radar measurement in the boreholes.	19
Table 6-1	Reflectors identified from high frequency antenna measurement in borehole KA3147G01.	26
Table 6-2	Reflectors identified from high frequency antenna measurement in borehole KA3153G01.	27
Table 6-3	Reflectors identified from high frequency antenna measurement in borehole KK0025G01.	28
Table 6-4	Reflectors identified from high frequency antenna measurement in borehole KK0031G01.	30
Table 6-5	Reflectors identified from high frequency antenna measurement in borehole KK0037G01.	32
Table 6-6	Reflectors identified from high frequency antenna measurement in borehole KK0045G01.	34
Table 6-7	Reflectors identified from high frequency antenna measurement in borehole KK0051G01.	35
Table 6-8	Reflectors identified from high frequency antenna measurement in borehole KD0086G01.	37
Table 6-9	Reflectors identified from high frequency antenna measurement in borehole KD0092G01.	40

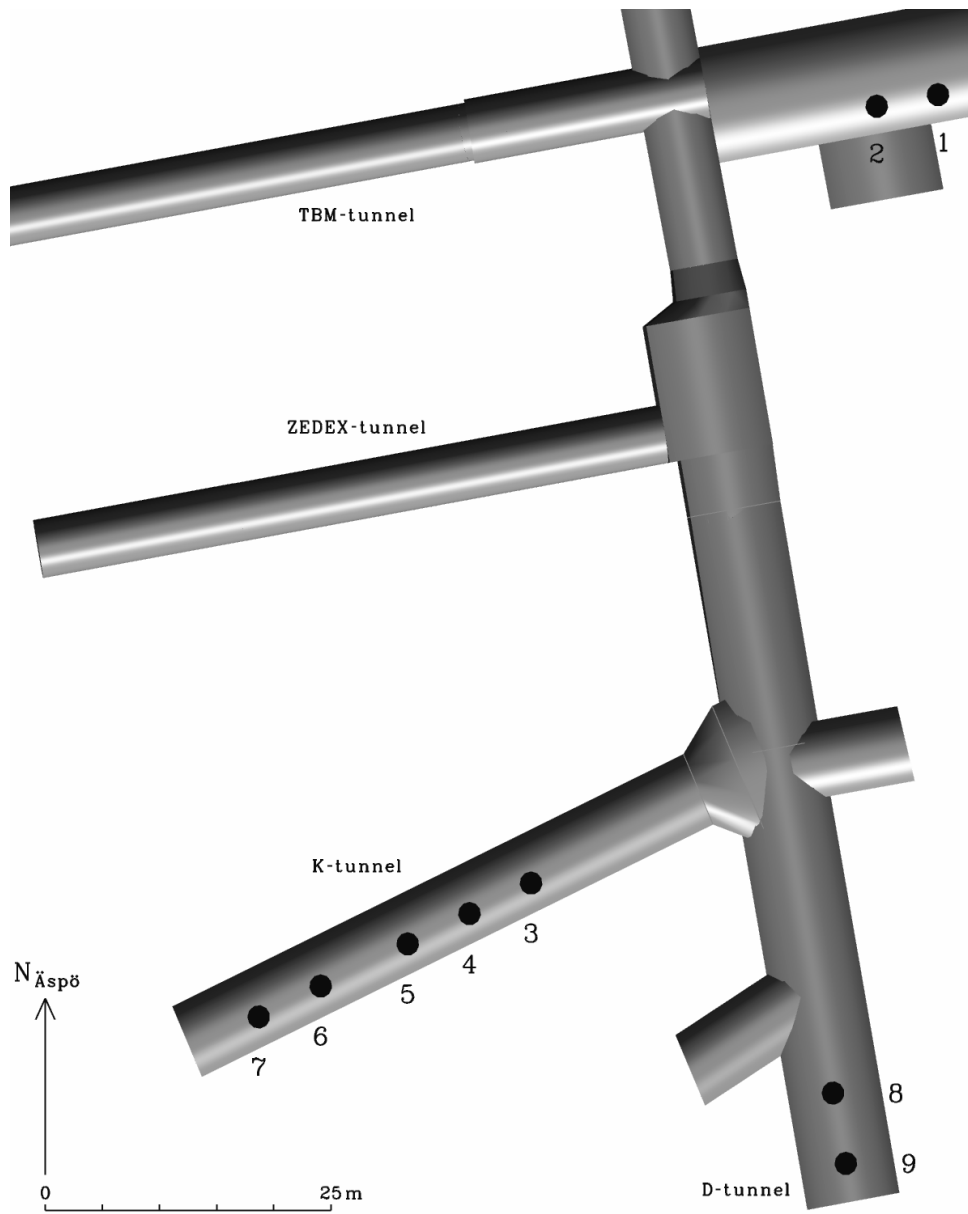
1 Introduction

The main aim of the borehole radar investigation reported here is to locate minor fracture zones and, as far as possible, single fractures. Attempts to orientate the reflectors are made by correlating the radar reflectors with structures from BIPS-mapping. The nine boreholes have been drilled from the tunnel floor at the D-tunnel (2 boreholes), K-tunnel (5 boreholes) and at the TBM-hall (2 boreholes).

The boreholes are drilled vertically down to a length of 8 m, except for borehole KK0045G01 which was drilled to a length of 8.5 m. Borehole data are presented in Table 1-1 and location of the boreholes in the tunnel is shown in Figures 1-1 and 1-2.

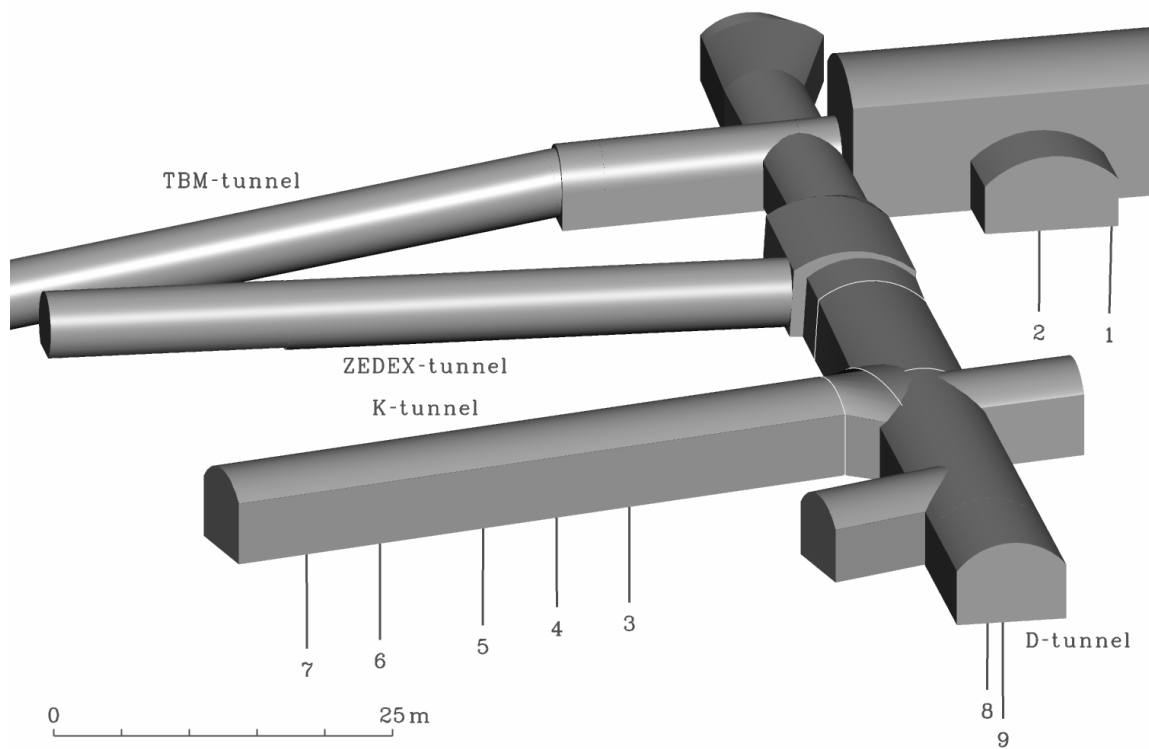
Table 1-1 Borehole data for the radar investigated boreholes included in the Demonstration of Deposition Technology Project. All values are given in the Äspö local system and in relation to Äspö local north. Data has been provided by SKB.

Borehole	X	Y	Z	Azimuth (degrees)	Dip (degrees)	Length (m)	Ø (mm)
KA3147G01	7312.490	2313.554	-419.561	253.7	-88.6	8.00	76
KA3153G01	7311.511	2308.194	-419.053	206.6	-89.7	8.00	76
KK0025G01	7245.576	2277.937	-417.189	180.0	-89.8	8.00	76
KK0031G01	7242.990	2272.551	-416.628	123.7	-89.6	8.00	76
KK0037G01	7240.417	2267.145	-417.066	191.3	-89.7	8.00	76
KK0045G01	7236.839	2259.527	-416.356	135.0	-89.8	8.50	76
KK0051G01	7234.226	2254.108	-416.592	108.4	-89.6	8.05	76
KD0086G01	7227.757	2304.366	-417.374	270.0	-89.9	8.00	76
KD0092G01	7221.789	2305.491	-417.384	135.0	-89.7	8.00	76



- | | |
|---------------|---------------|
| 1 = KA3147G01 | 6 = KK0045G01 |
| 2 = KA3153G01 | 7 = KK0051G01 |
| 3 = KK0025G01 | 8 = KD0086G01 |
| 4 = KK0031G01 | 9 = KD0092G01 |
| 5 = KK0037G01 | |

Figure 1-1 Location of radar measured boreholes.



- | | |
|---------------|---------------|
| 1 = KA3147G01 | 6 = KK0045G01 |
| 2 = KA3153G01 | 7 = KK0051G01 |
| 3 = KK0025G01 | 8 = KD0086G01 |
| 4 = KK0031G01 | 9 = KD0092G01 |
| 5 = KK0037G01 | |

Figure 1-2 Location of radar measured borehole. Looking towards Äspö local north.

2 Objectives

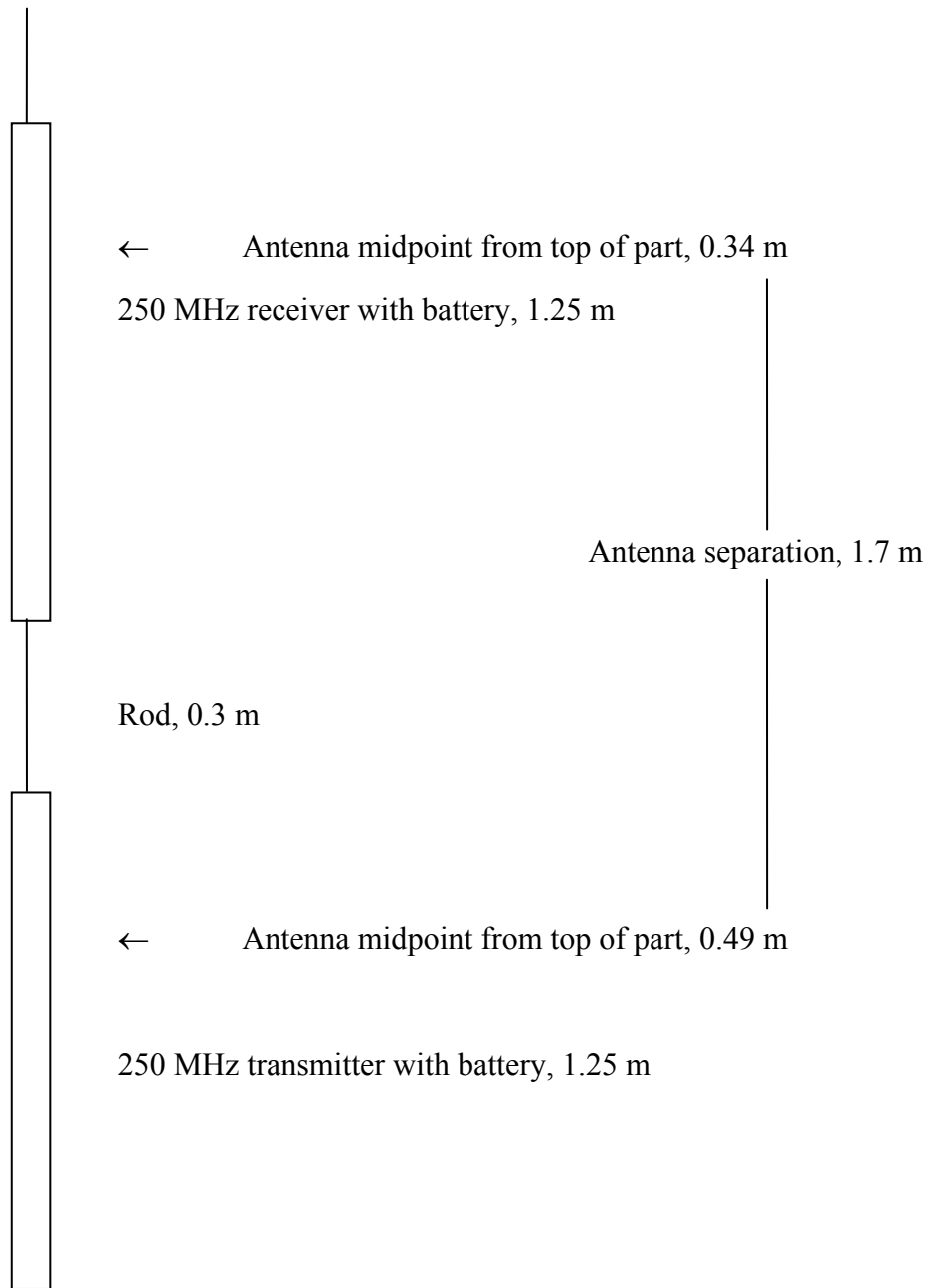
Borehole radar measurements using 250 MHz high frequency antenna have been performed in 9 cored boreholes drilled downwards from the floor in the D-tunnel, K-tunnel, and the TBM-hall. The objective was to find the location and map the extent of minor fracture zones and, as far as possible, single fractures intersecting the borehole. It should be noted that the high frequency antenna gives information about the intersection length and the angle between reflector and borehole axis, but no information about the direction (azimuth) to the reflectors relative the borehole.

3 Equipment used

The borehole radar measurements with high frequency antenna were performed using the RAMAC/GPR system.

The configuration of the high frequency equipment is shown in Figure 3-1.

Upward in borehole



Downward in borehole

Figure 3-1 Equipment configuration used for the high frequency radar measurement in the boreholes.

4 Data acquisition

Details of the measurements are given in Table 4-1.

Table 4-1 Specification of borehole radar measurement in the boreholes.

General

Type of measurement:	High frequency antenna, singlehole reflection mode.
Center frequency:	250 MHz
Transmitter-receiver separation:	1.7 m
Sampling frequency:	2646.88 MHz
No. of samples:	512
No. of stackings:	64
Equipment serial no.:	GPR/BH 250 MHz

Specific

Borehole KA3147G01

Surveyed borehole length:	1.15-6.06 m
Depth increment:	0.049 m
No. of records:	102
Date of measurement:	980424

Borehole KA3153G01

Surveyed borehole length:	1.15-6.15 m
Depth increment:	0.049 m
No. of records:	101
Date of measurement:	980424

Borehole KK0025G01

Surveyed borehole length:	1.15-6.06 m
Depth increment:	0.049 m
No. of records:	102
Date of measurement:	980424

Borehole KK0031G01

Surveyed borehole length:	1.15-6.16 m
Depth increment:	0.049m
No. of records:	104
Date of measurement:	980424

Borehole KK0037G01

Surveyed borehole length:	1.15-6.16 m
Depth increment:	0.049m
No. of records:	104
Date of measurement:	980424

Borehole KK0045G01

Surveyed borehole length: 1.15-6.45 m
Depth increment: 0.049m
No. of records: 110
Date of measurement: 980424

Borehole KK0051G01

Surveyed borehole length: 1.15-6.25 m
Depth increment: 0.049m
No. of records: 106
Date of measurement: 980424

Borehole KD0086G01

Surveyed borehole length: 1.15-6.11 m
Depth increment: 0.049 m
No. of records: 103
Date of measurement: 980424

Borehole KD0092G01

Surveyed borehole length: 1.15-6.16 m
Depth increment: 0.049 m
No. of records: 101
Date of measurement: 980424

5 Data processing

Reflectors have been identified in the DC-filtered and bandpass-filtered data. DC filtering corrects for voltage variations during measurement and sets all traces into an equal voltage level. Bandpass filtering is used to reduce disturbances such as high frequency ringing in the original radar data.

As a complement to the bandpass filtered radar map, moving-average filtered data was used for the interpretation. The moving-average filter reduces parallel features in the radar map such as parallel bands caused by ringing of the radar pulse. Moving-average filtering strengthens reflectors having a very steep angle to borehole axis.

The angle of intersection relative to the borehole (α -angle) and the intersection length with borehole have been determined for all identified reflectors. It is not possible to derive the absolute orientation of the respective reflectors.

Velocity calibration has earlier been performed in borehole KI0023B using the 250 MHz high frequency equipment. A measurement was made by having the 250 MHz transmitter fixed at 11 m in the borehole and the 250 MHz receiver moved from 10 m to 1 m in the borehole during measurement. The velocity was determined by comparing the difference in arrival time at different transmitter-receiver distances of the direct radar wave travelling along the borehole wall. With the velocity calibration as basis was the calculated velocity of radar waves in the borehole found to be 123 m/ μ s.

6 Results

6.1 General

The high frequency radar maps for the boreholes are shown as DC-filtered and bandpass filtered maps and also as moving-average filtered maps. The interpretation of radar reflectors from the boreholes is shown in figures as interpretation maps.

The result from the high frequency antenna measurements in the boreholes is shown in a separate appendix. The appendix contains the DC-filtered and bandpass filtered maps, the moving-average filtered maps, and the interpretation maps.

The interpretation of the radar measurements has been made using the computer program RADINTER.

The reflectors identified from the high frequency antenna measurements in the boreholes are listed in tables. The tables for the holes also contain correlation with BIPS-structures. Orientations of structures as interpreted from BIPS-logging are presented in the tables.

The depth of intersection for reflectors with the borehole is given relative to the tunnel floor level. The accuracy of the listed intersection depth is ± 0.5 m for the high frequency reflectors.

Magnitude is a relative (subjective) measure on the strength of the reflectors on a scale from 1 to 3. A rating of 1 signifies a weak reflector and 3 a strong reflector. The abbreviation "U" signifies a reflector having a magnitude so weak that the existence of the reflector is uncertain. The abbreviation "A" indicates that the reflector has been identified in the moving-average filtered radar map.

Strike of BIPS-oriented reflectors is given relative to *Äspö local north*. Dip angles are in the interval 0 to 90 degrees, while strike directions are in the range 0 to 360 degrees. A strike of 0 degrees implies a dip to the Äspö local east while a strike of 180 degrees implies a dip to the Äspö local west. Strike angle is positive clockwise from Äspö local north.

6.2 High frequency antenna in the boreholes

Radar measurements with the 250 MHz antenna were performed in 9 boreholes drilled vertically downwards from the floor in the D-tunnel, the K-tunnel, and the TBM-hall. The boreholes were drilled to a depth of 8 m while borehole KK0045G01 was drilled to a depth of 8.5 m. The location of the boreholes is shown in Figures 1-1 and 1-2. The location and direction of the boreholes are based on data provided by SKB. Core logs and results from BIPS measurements, provided by SKB, have been used for correlation of radar reflectors with geology. Radar maps and interpretation maps for the boreholes are shown in an appendix.

The strongest radar reflectors are, as a general rule for the boreholes, observed in the upper part of the radar map in form of a couple of strong parallel features. The strong reflectors represent reflections from the tunnel floor and/or the tunnel roof. The parallel reflectors have not been indicated in the interpretation maps. Also, probably neighbouring boreholes can be seen in some of the radar maps in form of parallel reflectors.

The measured section length in the boreholes, which is generally around 5 m, is relatively short. A combination of the direct radar pulse travelling along the borehole wall and the ringing of the radar pulse, caused by the rather large borehole diameter (76 mm), creates a "blind" zone close to the borehole. In the radar map the "blind" zone is located between 0-1.5 m outside the borehole. The short measured section length in combination with the "blind" zone makes it difficult to detect structures intersecting the borehole with a small angle to borehole axis, especially if these reflectors are weak. However, strong reflectors with rather small angle to borehole axis can, for example, be observed in the radar map for boreholes KD0086G01 and KK0045G01.

In order to enhance reflections from structures intersecting the borehole axis at high angle has moving-average filtering been used. The moving-average filtered radar maps are presented in the appendix together with the bandpass filtered radar maps. The moving-average filter removes the ringing of the radar pulse and thereby reveals a large part of the "blind" zone mentioned above. It should be noted that reflectors having a small angle to borehole axis, i.e. reflectors more or less parallel to borehole axis are suppressed by this filtering method.

The bottom of the boreholes is generally indicated in the moving-average filtered radar maps by a reflector having an angle of 90° to borehole axis and interpreted to intersect the borehole ± 0.2 m from the exact position of the end-point of the borehole. This type of reflectors can be observed in most of the nine investigated boreholes.

The correlation between high frequency radar reflectors and geological structures mapped by BIPS is generally considered as good for the boreholes. The correlation is presented in the interpretation table for each individual borehole.

6.2.1 Results from measurement in KA3147G01

The radar map contains 12 reflectors of which 6 can be connected to single fractures or lithological contacts. Reflector 1 represents the tunnel floor, reflector 9 the bottom of the borehole, while reflectors 6 and 7 are interpreted to intersect below the end-point of the borehole. Most of the reflectors have been identified in the moving-average filtered radar map.

The lower limb of the weak reflector 2 at 1.6 m can be correlated with a greenstone at 1.6-1.9 m. The reflector is observed close to the borehole and can be traced to a distance of 3 m outside the borehole. The α -angle is 57° for the reflector and 55° for the BIPS-structure.

Reflectors 10, 3, and 4 are parallel to each other in the radar map. Reflector 10 at 2.5 m indicates a greenstone at 2.0-2.1 m. The angle to borehole axis of the reflector is 64° and the corresponding angle of the BIPS-structure is 65° . There are no suitable structures to be correlated with reflector 3 at 3.1 m or reflector 4 at 3.6 m.

The upper limb of the weak reflector 12 at 4.7 m occurs close to a section with fractures between 4.7-5.2 m. The reflector can be observed only over a short distance. The reflector can be correlated with one fracture at 5.0 m. Reflector 11 at 5.6 m is in the radar map parallel to reflector 12. Reflector 11 indicates a fracture at 5.3 m. The agreement between α -angles is very good.

Reflector 8 at 7.1 m and reflector 5 at 7.5 m are parallel to each other in the radar map. Reflector 8 occurs close to a fracture at 6.7 m and reflector 5 occurs at a section with fine-grained granite between 7.5-7.6 m. Both reflectors can be traced as straight lines in the radar map from the borehole to a distance of 5-6 m outside the borehole. The agreement between the angle for reflector 8, which is 83° , and the BIPS-structure, which is 36° , is not very good. However, the agreement between reflector 5 (90°) and the corresponding BIPS-structure (59°) is better.

Reflector 6 at 9.5 m and reflector 7 at 10.5 m are interpreted to intersect below the end-point of the borehole. Both reflectors can be observed as straight lines in the moving-average filtered radar map between the distance 3-5 m outside the borehole.

Table 6-1 Reflectors identified from high frequency antenna measurement in borehole KA3147G01.

Re-flec-tor ID	Depth of inter-section (m)	Angle of inter-section (degree)	Magnitude 1= weak 2= medium 3= strong U= uncertain A= moving average map	Position of geological structure (m)	Character of geological structure	Angle of inter-section of BIPS-structure (degree)	Orientation of BIPS-mapped structure
1	0.0	90	3		Floor		
2	1.6	57	1A	1.5	Greenstone	55	35/267
10	2.5	64	1A	2.7	Greenstone	65	25/053
3	3.1	70	2A	-	-		
4	3.6	69	2A	-	-		
12	4.7	70	1A	5.0	Fracture	63	27/119
11	5.6	75	1A	5.3	Fracture	77	13/060
8	7.1	83	2A	6.7	Fracture	36	54/001
5	7.5	90	2	7.5-7.6	Red fine-grained granite	59	31/313
9	8.0	90	2A		Bottom		
6	9.5	89	1		Below		
7	10.5	66	2		Below		

6.2.2 Results from measurement in KA3153G01

The radar map shows 11 reflectors that have been identified in the moving-average filtered radar map as well as in the bandpass filtered radar map. Reflector 1 is interpreted to represent the tunnel floor and reflector 7 is indicating the bottom of the borehole.

Of the 11 reflectors have 6 been connected to different geological features, such as single fractures and lithological contacts. Two reflectors, reflector 8 at 9.2 m and 9 at 10.0 m, have both been interpreted to intersect below the end-point of the borehole.

The lower limb of the weak reflector 2 at 0.9 m with the angle 70° is observed close to the borehole. There is a fracture at 0.7 m having the angle 73° to borehole axis.

The lower limb of reflector 3 at 1.7 m is observed close to the borehole and further out to a distance of 2 m from the borehole. There is greenstone in a section between 1.85-1.95 m, according to the core log. The angle of the reflector is 63° and the angle of the BIPS-structure is 43°.

Reflector 4 at 2.6 m is also weak in the radar map. The lower limb can be traced from the borehole to a distance of 2.5 m outside the borehole. The reflector intersects the borehole at a lithological contact between greenstone and småland granite at 2.75 m. The angle of the radar reflector is 71° and the angle of the BIPS-structure is 43°.

Reflector 11 occurs at 5.4 m having the angle 62° to borehole axis. There is a fracture at 5.15 m according to the core log. The BIPS-angle of the fracture is 22° and the agreement between radar reflector and BIPS-structure is not good.

The upper limb of reflector 5 at 6.5 m is weak but can although be traced from the borehole to a distance of almost 5 m outside the borehole. The reflector intersects the borehole close to a fracture at 6.9 m. The angle of the reflector is 79° and the angle of the BIPS-structure is 74°.

Reflector 6 at 7.5 m and reflector 10 at 7.8 m both have the angle 90° to borehole axis. The reflectors are strong in the radar map and can be traced from the borehole to a distance of at least 4-5 m outside the borehole. Both reflectors indicate a section of red fine-grained granite located from 7.5 m to the end of the borehole. The BIPS-interpreted angle of the upper contact is 53°.

Table 6-2 Reflectors identified from high frequency antenna measurement in borehole KA3153G01.

Re- flec- -tor ID	Depth of inter- section (m)	Angle of inter- section (degree)	Magnitude 1= weak 2= medium 3= strong U= uncertain A= moving average map	Position of geological structure (m)	Character of geological structure	Angle of inter- section of BIPS- structure (degree)	Orientation of BIPS- mapped structure
1	-0.1	90	3		Floor		
2	0.9	70	1A	0.7	Fracture	73	17/127
3	1.7	63	1A	1.85-1.95	Greenstone	43	47/054
4	2.6	71	1A	2.75	Greenstone/ småland granite	43	47/034
11	5.4	62	1A	5.15	Fracture	22	68/314
5	6.5	79	1A	6.9	Fracture	74	16/019
6	7.5	90	3	7.5-8.0	Red fine- grained granite	53	37/197
10	7.8	90	3A	7.5-8.0	Red fine- grained granite	-	
7	8.2	90	3		Bottom		
8	9.2	60	3		Below		
9	10.0	56	3A		Below		

6.2.3 Results from measurement in KK0025G01

The bandpass filtered and the moving-average filtered radar maps from this borehole contains 8 reflectors. Reflector 1 is interpreted to represent the tunnel floor while reflector 7 is indicating the bottom of the borehole. Six of the reflectors can be connected to geological features in the borehole such as lithological contacts or fractures.

Reflector 8 at 1.0 m has the angle 55° to borehole axis and occurs close to a lithological contact between greenstone and diorite at 0.8 m and also close to a fracture at 10.3 m. The α -angle of the lithological contact is 37° and it is 31° of the fracture. It is difficult to decide which of the structures that can be connected to the radar reflector.

The lower limb of reflector 2 at 2.5 m can be observed in the radar map from the borehole to a distance of 3 m outside the borehole. The α -angle of the reflector is 49°. There are two possible candidates to reflector 2, one is a fracture at 2.85 m with the angle 28° and the other is a fracture at 2.9 m with the angle 37°. However, best fitness between radar reflector and fracture is achieved with the angle 37°.

Reflectors 3 at 4.3 m, 4 at 5.4 m, and 5 at 6.0 m are weak and parallel to each other in the radar map. They are observed from the borehole to a distance of 2-3 m outside the borehole. Reflector 3 occurs close to a pegmatite at 3.8-3.9 m. The α -angle is 66° for the BIPS-structure and 78° for the radar reflector. Reflector 4 with the BIPS-interpreted angle 65° occurs close to a contact between greenstone and diorite at 5.95 m with the angle 64°, and a fracture at 5.15 m with the BIPS-interpreted angle 26°. Best fitness is achieved with the lithological contact. Reflector 5 at 6.0 m has the angle 78°. Reflector 5 occurs close to a contact between greenstone and diorite at 6.15 m. The BIPS-interpreted angle for the contact is 62°.

The upper limb of reflector 6 at 7.4 m can be seen close to the borehole. There is a contact between diorite and småland granite at 7.65 m, according to the preliminary core log. However, this part of the borehole was not logged with BIPS.

Table 6-3 Reflectors identified from high frequency antenna measurement in borehole KK0025G01.

Re- Flec Tor ID	Depth of inter- section (m)	Angle of inter- section (degree)	Magnitude 1= weak 2= medium 3= strong U= uncertain A= moving average map	Position of geological structure (m)	Character of geological structure	Angle of inter- section of BIPS- structure (degree)	Orientation of BIPS- mapped structure
1	0.1	90	3		Floor		
8	1.0	55	1A	0.8	Greenstone	37	53/172
				1.3	Fracture	31	59/198
2	2.5	49	2A	2.85	Fracture	28	62/195
				2.90	Fracture	37	53/202
3	4.3	78	1A	3.8-3.9	Pegmatite	66	24/281
4	5.4	65	1A	5.15	Fracture	26	64/269
				5.95	Contact greenstone/ diorite	64	26/291
5	6.0	78	1	6.15	Contact greenstone/ diorite	62	28/342
6	7.4	54	1	7.65	Contact diorite/ småland granite	-	
7	7.9	90	2A		Bottom		

6.2.4 Results from measurement in KK0031G01

The radar map contains 11 reflectors. Reflector 1 is indicating the tunnel floor and reflector 7 the bottom of the borehole.

The bandpass filtered radar map contains two rather prominent reflectors, reflector 8 at 8.7 m and 10 at 10.4 m, which both are interpreted to intersect below the end-point of the borehole. Reflector 8 can be traced as a straight line across the radar map, starting near the borehole to a distance of about 5 m outside the borehole. The structure which reflector 8 represents should be found at the tunnel floor in a radius of 8-9 m around the borehole. Reflector 10 can be traced as a straight line from 2 m outside the borehole to a distance of 6 m outside the borehole. The structure which reflector 10 indicates should be found in the tunnel floor in a radius of 13-14 m around the borehole.

The moving-average filtered radar map contains 6 reflectors that are interpreted to intersect the borehole. The 6 reflectors can be connected to geological features in the borehole, such as lithological contacts or fracturing. The reflectors are rather weak and can be traced from the borehole to a distance of 2-3 m outside the borehole

Reflector 2 is interpreted to intersect at 0.2 m. The lower limb can be traced from the borehole to a distance of at least 3 m outside the borehole. The reflector has an angle of 45° and it occurs close to a lithological contact at 0.5 m between diorite and småland granite. The BIPS-interpreted angle of the contact is 37° .

The lower limb of the weak reflector 3 at 1.4 m can be observed from the borehole to a distance of about 3 m outside the borehole. The reflector occurs close to a greenstone between 1.6-1.7 m. The radar angle is 64° and the α -angle interpreted from the BIPS-logging is 46° .

Reflector 4 at 4.4 m also exhibits a weak character in the radar map. The reflector can be observed close to the borehole. The angle to borehole axis of the reflector is 66° . The reflector can be correlated with a fracture at 3.6 m having the angle 75° to borehole axis or with a greenstone at 4.0 m having the angle 40° . The difference between interpreted intersection length of the reflector and the fracture is rather large, but the agreement between α -angles is good. Best fitness is probably achieved with the greenstone, although the difference in α -angles is rather large.

The upper limb of reflector 5 at 6.0 m is weak and can be seen close to the borehole. The core log shows sealed fracture at 6.35 m with the α -angle 47° . The corresponding angle of the radar reflector is 45° .

Reflector 6 at 6.9 m and reflector 11 at 7.1 m occur close to each other. Reflector 6 with the angle 90° can be correlated with a fracture at 6.85 m having the angle 86° . The core log shows greenstone between 7.0-7.15 m and a fracture at 7.15 m close to the interpreted intersection length for reflector 11. It is difficult to decide if reflector 11 represents the greenstone or the fracture. The BIPS-interpreted α -angle of the greenstone is 23° and the angle of the fracture is 24° .

Reflector 9 is weak and intersects the borehole at 8.9 m, i.e. below the end-point of the borehole.

Table 6-4 Reflectors identified from high frequency antenna measurement in borehole KK0031G01.

Reflec- tor ID	Depth of inter- section (m)	Angle of inter- section (degree)	Magnitude 1= weak 2= medium 3= strong U= uncertain A= moving average map	Position of geological structure (m)	Character of geological structure	Angle of inter- section of BIPS- structure (degree)	Orienta- tion of BIPS- mapped structure
1	0.1	90	3		Floor		
2	0.2	45	2A	0.5-0.8	Småland granite	37	53/343
3	1.4	64	1A	1.6-1.7	Greenstone	46	44/320
4	4.4	66	1A	3.6	Fracture	75	15/267
				4.0	Greenstone	40	50/016
5	6.0	45	1A	6.35	Sealed fracture	47	43/283
6	6.9	90	1A	6.85	Fracture	86	4/034
11	7.1	37	1A	7.05-7.15	Greenstone	23	67/025
				7.15	Fracture	24	66/249
7	8.0	90	1A		Bottom		
8	8.7	44	3		Below		
9	8.9	76	1A		Below		
10	10.4	54	2		Below		

6.2.5 Results from measurement in KK0037G01

A total of 13 reflectors has been interpreted from the radar map. Besides the strong parallel reflectors connected to the tunnel floor and also probably to the tunnel roof, can one prominent reflector be identified in the bandpass filtered radar map. Reflector 1, which has a strong magnitude in the radar map, differs from the other reflectors by being parallel to the borehole axis. The reflector is calculated to intersect above the borehole top, i.e. it should be found at the tunnel floor in a radius of 3-4 m around the borehole. It is possible that the reflector indicates a nearby borehole.

Reflector 2 is best observed in the moving-average filtered radar map. The reflector has an undulating character in the radar map and is interpreted to intersect above the top of the borehole, or in a radius of 1-2 m around the borehole.

Reflector 3 indicates the tunnel floor.

The moving-average filtered radar map contains 7 reflectors that are interpreted to intersect the borehole. The reflectors can be correlated to geological features in the borehole such as lithological contacts or fractures.

The upper limb of reflector 4 at 2.9 can be observed over a short distance close to the borehole. The reflector occurs at a section of småland granite between 2.6-2.75 m. The BIPS-interpreted α -angle for the småland granite is 36° and the corresponding angle of the radar reflector is 46° .

Reflector 5 at 3.5 m is observed in the radar map by its lower limb. The magnitude of the reflector is small and it can be seen close to the borehole. There are several sealed fractures at this depth. Best fitness is achieved with a fracture at 3.3 m, which has the α -angle 36° . The angle of the radar reflector is 73° , i.e. the agreement is not good.

Reflector 6 at 4.2 m is also a reflector having a weak character in the radar map. The reflector intersects the borehole at a section of greenstone between 4.45-4.5 m. The angle of the radar reflector is 66° and the BIPS-interpreted angle of the greenstone is 52° .

The upper limb of reflector 7 can be observed in the moving average map. The reflector is weak and the intersection with borehole is interpreted to be at 5.2 m. There is a sealed fracture at 5.2 m, according to the core log. The α -angle from the BIPS-interpretation is 20° and the corresponding angle of the radar reflector is 48° .

Reflectors 8 at 6.6 m and 9 at 7.8 m are parallel to each other in the radar map. Both reflectors exhibit an undulating character in the radar map. This makes the exact interpretation of intersection with borehole uncertain. The reflectors can be traced from the borehole to a distance of 3 m outside the borehole. Reflector 8 indicates a greenstone between 6.3-6.35 m. The BIPS-interpreted angle of the greenstone is 44° and the angle of the radar reflector is 46° . Reflector 9 intersects the borehole below the BIPS logged section, and the core log shows no suitable structures at this depth.

Reflector 13 can be seen close to the borehole as a weak line in the moving-average filtered radar map. The intersection with borehole is at 7.0 m and the angle to borehole axis is 31° . The core log shows two possible candidates, namely the lithological contact between diorite and greenstone at 6.6 m and a fracture at 6.8 m. The BIPS-interpreted α -angle of the lithological contact is 32° and the α -angle of the fracture is 39° . Corresponding angle for the radar reflector is 31° .

Reflector 10 at 8.8 m, reflector 11 at 9.0 m, and reflector 12 at 11.4 m are parallel to each other in the radar map. They are interpreted to intersect below the end-point of the borehole. The reflectors are best observed in the moving-average filtered radar map. The reflectors, which exhibit rather straight characters in the radar map, can be observed from 1-3 m outside the borehole to a distance of 5-6 m from the borehole.

Table 6-5 Reflectors identified from high frequency antenna measurement in borehole KK0037G01.

Re- flec tor ID	Depth of inter- section (m)	Angle of inter- section (degree)	Magnitude 1= weak 2= medium 3= strong U= uncertain A= moving average map	Position of geological structure (m)	Character of geological structure	Angle of inter- section of BIPS- structure (degree)	Orientation of BIPS- mapped structure
1	-95	2	3	In a radius of 3-4 m around the borehole			
2	-2	25	1A	In a radius of 1-2 m around the borehole			
3	0.2	90	3		Floor		
4	2.9	46	2A	2.6-2.75	Småland granite	42	48/020
5	3.5	73	1A	3.3	Sealed fracture	36	54/264
6	4.2	66	1A	4.45-4.5	Greenstone	52	38/065
7	5.2	48	1A	5.2	Sealed fracture	20	70/284
8	6.6	46	2A	6.3-6.35	Greenstone	44	46/038
13	7.0	31	1A	6.6	Diorite/ greenstone	32	58/050
9	7.8	37	2A	6.8	Fracture	39	51/014
10	8.8	41	3	-	Below	-	
11	9.0	49	2A		Below		
12	11.4	40	1A		Below		

6.2.6 Results from measurement in KK0045G01

Almost all 14 interpreted reflectors in this borehole have been identified in the moving-average filtered radar map. Of them are 7 reflectors interpreted to intersect the borehole and all of them have been correlated with geological structures such as lithological contacts or fractures. The strong reflector 1 is more or less parallel to borehole axis. It can be seen in the radar map as a straight line at a distance of 2-3 m outside the borehole, and it should be found in the tunnel floor in a radius of 2-3 m around the borehole.

The strong reflector 2 at 0.0 m represents the tunnel floor.

Reflector 3 at 0.4 m exhibits an undulating character in the moving-average filtered radar map. The exact intersection with borehole is thereby somewhat uncertain. It is likely that the reflector indicates the contact between greenstone and red fine-grained granite at 0.5 m. The reflector can be traced from the borehole to a distance of 4-5 m outside the borehole. The BIPS-interpreted α -angle is 65° and the corresponding angle for the radar reflector is 51° .

Reflector 4 at 1.8 m also exhibits an undulating shape in the moving-average radar map. There is a lithological contact at 1.65 m between diorite and greenstone having the α -angle 33° and a pegmatite at 1.9 m having the angle 40° . The radar reflector has an angle of 52° and the best fitness with structures in the borehole is achieved with the pegmatite.

Reflector 5 at 2.1 m probably indicates a pegmatite at 2.05 m. The reflector can be seen to a distance of 2 m outside the borehole where it seems to change direction (reflector +5). The α -angle of the BIPS-interpreted pegmatite is 36° and the angle of the radar reflector is 44° .

Reflector 6 at 3.5 m is weak in the radar map. The lower limb of the reflector can be observed over a short distance, starting at the borehole and continuing to a distance of 2.5 m from the borehole. There is a fracture at 3.5 m. The BIPS-interpreted α -angle is 24° and the angle of the radar reflector is 53° , i.e. the correlation between α -angles is not very good.

The upper limb of reflector 7 at 4.6 m is clearly visible in the radar map. The reflector can be observed as a straight line from the borehole to a distance of about 2 m outside the borehole. The reflector is interpreted to intersect the borehole within a section of pegmatite between 4.2-4.9 m. The BIPS-interpreted α -angle of the pegmatite is 44° and the corresponding angle of the radar reflector is 50° .

The upper limb of reflector 8 at 5.9 m can be observed as a straight line from the borehole to a distance of at least 3 m outside the borehole. The reflector indicates the contact at 5.65 m between diorite and greenstone. The α -angle of the contact is 75° and the angle of the radar reflector is 51° . The agreement between angles is not very good, but acceptable.

The interpretation of reflector 9 at 7.2 m is uncertain due to the small magnitude of the reflector. The core log shows the presence of red fine-grained granite at 7.05-7.1 m. BIPS-interpretation shows the α -angle 18° for the granite, and corresponding angle for the radar reflector is 54° , i.e. the agreement between angles is not very good.

Reflector 10 at 8.2 m indicates the bottom of the borehole.

Reflectors 11, 12, 13, and 14 are parallel to each other in the radar map. They are all interpreted to intersect below the end-point of the borehole. They can be observed from 2 m to almost 7 m outside the borehole.

Table 6-6 Reflectors identified from high frequency antenna measurement in borehole KK0045G01.

Re-flec-tor ID	Depth of inter-section (m)	Angle of inter-section (degree)	Magnitude 1= weak 2= medium 3= strong U= uncertain A= moving average map	Position of geological structure (m)	Character of geological structure	Angle of inter-section of BIPS-structure (degree)	Orientation of BIPS-mapped structure
1	-238	1	3	In a radius between 2-3 m around borehole			
2	0	90	3		Floor		
3	0.4	51	1A	0.0-0.5	Contact greenstone/ red fine-grained granite	65	25/104
4	1.8	52	1A	1.65	Contact diorite/ greenstone	33	57/307
5	2.1	44	1A	1.9	Pegmatite	40	50/205
+5	2.8	55	1A	2.05	Pegmatite	36	54/218
6	3.5	53	1A	-			
7	4.6	50	2A	3.5	Fracture	24	66/052
8	5.9	51	2A	4.2-4.9	Pegmatite	44	46/160
9	7.2	54	1UA	5.65	Contact diorite/ greenstone	75	15/196
10	8.2	90	2A	7.05-7.1	Red fine-grained granite	18	72/189
11	9.4	41	1A		Bottom		
12	10.5	38	2A		Below		
13	12.2	44	1		Below		
14	12.3	54	1		Below		

6.2.7 Results from measurement in KK0051G01

A total of 11 radar reflectors has been identified in the radar map. The strong reflector 1 is representing the tunnel floor and the strong reflector 7 is representing the bottom of the borehole. Of the 11 reflectors can 6 be connected with geological structures in the borehole.

The lower limb of reflector 2 at 0.7 m can be traced from the borehole to a distance of 4 m outside the borehole. The reflector indicates either a greenstone between 0.65-0.75 m or a pegmatite at 0.9 m. The angle of the radar reflector is 46°. Interpretation from BIPS-logging shows that the corresponding angle for the greenstone is 19° and for the pegmatite it is 34°. Best agreement between radar reflector and structures in the borehole is achieved with the pegmatite.

The lower limb of reflector 11 is rather strong in the moving-average filtered radar map and can be observed from the borehole to a distance of 3.5 m outside the borehole. The reflector is interpreted to intersect the borehole at 1.2 m having the angle 44° to borehole axis. There is greenstone between 1.25-1.35 m, according to the core log. Results from BIPS-interpretation show that the α -angle for the greenstone is 44°.

Reflector 3 is prominent in the moving average filtered radar map. Calculated intersection with borehole is at 2.0 m, but the undulating character of the reflector might result in an intersection above this borehole length. The lower limb of reflector 3 can be traced from the borehole to a distance of 3.5 m outside the borehole. There is pegmatite at 1.85 m and the angle to borehole axis of the pegmatite is 63°. The corresponding angle of the radar reflector is 49°.

Reflector 4 at 3.4 m is in the radar map parallel to reflector 3. The character of the reflector is similar to that of reflector 3 above. The reflector indicates sealed epidote fractures at 3.4 m. The angle to borehole axis of the radar reflector is 55° and the corresponding angles for the sealed fractures are 36° and 35°, respectively.

Reflector 5 at 6.7 m has a small magnitude in the radar map. There is a fracture at 6.25 m that can be correlated with the radar reflector. The angle to borehole axis of the radar reflector is 55° and the BIPS-interpreted α -angle of the fracture is 32°.

The upper limb of reflector 6 at 7.3 m also exhibits a small magnitude in the radar map. The angle to borehole axis of the reflector is 90°. The reflector is correlated with a fracture at 7.55 m that has the α -angle 86°, according to the BIPS-interpretation.

Reflectors 8, 9, and 10 are interpreted to intersect below the end-point of the borehole. The three reflectors can be traced over appreciable distances in the radar map.

Table 6-7 Reflectors identified from high frequency antenna measurement in borehole KK0051G01.

Re- flec- tor ID	Depth of inter- section (m)	Angle of inter- section (degree)	Magnitude 1= weak 2= medium 3= strong U= uncertain A= moving average map	Position of geological structure (m)	Character of geological structure	Angle of inter- section of BIPS- structure (degree)	Orientation of BIPS- mapped structure
1	0.2	90	3		Floor		
2	0.7	46	1	0.65-0.75	Greenstone	19	71/042
				0.9	Pegmatite	34	56/023
11	1.2	44	2A	1.25-1.35	Greenstone	44	46/032
3	2.0	49	3A	1.85	Pegmatite	63	27/001
4	3.4	52	2A	3.4	Sealed epidote fractures	36 35	54/228 55/245
5	6.7	55	1A	6.25	Fracture	32	58/282
6	7.3	90	1A	7.55	Fracture	86	4/079
7	8.1	90	3		Bottom		
8	9.6	43	2		Below		
9	9.9	53	1A		Below		
10	11.1	28	3		Below		

6.2.8 Results from measurement in KD0086G01

A total of 11 reflectors has been interpreted from the radar map. Of them are 6 reflectors correlated with geological structures.

Reflector 1 is prominent in the radar map. The reflector, which is parallel to the borehole axis, represents a structure or a borehole, which should be found in the tunnel floor in a radius of 4-5 m around the borehole. The reflector can be traced from the top to the bottom of the radar map.

Reflector 2 is also prominent in the radar map. The reflector has an angle of 62° to borehole axis, and is interpreted to intersect above the top of the borehole, i.e. in a radius of 0-1 m around the borehole. The reflector can be traced as a straight line from the borehole to a distance of 6 m outside the borehole.

Reflector 11 is weak in the radar map. The angle to borehole axis is 19° and the reflector is interpreted to intersect above the borehole top. Calculations show that it should be found in the tunnel floor in a radius of 0-1 m around the borehole.

The lower limb of reflector 3 is prominent in the moving-average filtered radar map. The reflector can be traced from a distance of 4 m outside the borehole and almost into the borehole at the intersection length 1.3 m, even if the reflector is weak close to the borehole. There is a fracture at 1.1 m and a quartz vein at 1.35-1.4 m, according to the core log. The angle to borehole axis of the radar reflector is 46° . Corresponding α -angle interpreted from the BIPS-logging is 32° for the fracture and 20° for the quartz vein. Best fitness is achieved with the fracture.

The lower limb of reflector 10 at 3.3 m can be observed at a rather short extension in the radar map, i.e. from 1.5 m to 3 m from the borehole. There is a fracture at 2.7 m having the α -angle 37° and a section with greenstone between 3.0-3.5 m with the α -angle 5° . The α -angle of the radar reflector is 61° . Best fitness between radar reflector and BIPS-structure is achieved with the fracture, even if there is a large difference between the α -angles.

The lower limb of the weak reflector 4 at 4.3 m has a short extension in the moving-average filtered radar map. Three possible candidates for correlation have been found in the core log. There is pegmatite between 3.85-3.90 m and the BIPS-interpreted α -angle is 35° . Then there is greenstone between 3.9-4.0 m with the α -angle 27° . Finally, there is a lithological contact between fine-grained granite and diorite at 4.05 m and the α -angle is 47° . Both borehole length and α -angle for the lithological contact suit radar reflector 4 at 4.3 m, which has the angle 43° to borehole axis.

The upper limb of reflector 5 at 6.1 m can be seen in the moving-average map as a weak but straight line from the borehole to a distance of almost 3 m outside the borehole. There is a narrow section of pegmatite between 6.20-6.25 m according to the core log. Interpretation from BIPS-logging shows that the α -angle of the pegmatite is 59° . This is in agreement with the corresponding angle of the radar reflector, which is 45° .

Reflector 6 is rather prominent in the moving-average filtered radar map and the upper limb of the reflector can easily be traced in the radar map from the intersection with borehole at 6.7 m and continuing outside to a distance of almost 5 m from the borehole. The reflector probably indicates a pegmatite between 6.45-6.50 m. Interpretation from

BIPS-logging shows that the angle to borehole axis of the pegmatite should be 73°. Corresponding angle of the radar reflector is 65°.

Reflector 7 at 7.3 m has a weak appearance in the radar map. The upper limb can be seen as a weak but straight line from 2 m to 3 m away from the borehole. At this distance the strong reflector 2 covers reflector 7. The core log shows a fracture at 7.5 m. Interpretation from BIPS shows the α -angle 12° for the fracture, while the corresponding angle for the radar reflector is 34°. The difference between the angles is relatively large.

The rather prominent reflectors 8 and 9 are both interpreted to intersect below the end-point of the borehole. The upper limbs of the reflectors can be observed as straight lines from 1-2 m outside the borehole to a distance of 5-6 m from the borehole.

Table 6-8 Reflectors identified from high frequency antenna measurement in borehole KD0086G01.

Re-flec- tor ID	Depth of inter- section (m)	Angle of inter- section (degree)	Magnitude 1= weak 2= medium 3= strong U= uncertain A= moving average map	Position of geological structure (m)	Character of geological structure	Angle of inter- section of BIPS- structure (degree)	Orientation of BIPS- mapped structure
1	-1.72	1	3	At floor in a radius of 4-5 m around the borehole	Nearby borehole?		
2	-0.5	62	3	At floor in a radius of 0-1 m around the borehole			
11	-0.4	19	1A	At floor in a radius of 0-1 m around the borehole			
3	1.3	46	3	1.1 1.35-1.40	Fracture Quartz 50 mm	32 20	58/002 70/343
10	3.3	61	1A	2.7 3.0-3.5	Fracture Greenstone	37 5	53/022 85/208
4	4.3	43	1A	3.85-3.90 3.90-4.0 4.05	Pegmatite Greenstone Contact red fine-grained granite/diori te	35 27 47	55/194 63/193 43/094
5	6.1	45	1A	6.20-6.25	Pegmatite	59	31/281
6	6.7	65	3A	6.45-6.50	Pegmatite	73	17/350
7	7.3	34	1A	7.5	Fracture	12	78/351
8	8.5	60	2A		Below		
9	9.7	51	2A		Below		

6.2.9 Results from measurement in KD0092G01

A total of 11 reflectors has been interpreted from the radar map. Of these are 7 reflectors interpreted to intersect the borehole.

The lower limb of reflector 1 is prominent in the radar maps. The reflector indicates the tunnel floor.

Reflector 10 is rather prominent and can be traced across the radar map from the bottom to the top. The reflector exhibits an undulating shape ($40\text{-}50^\circ$ to borehole axis) and the intersection with borehole is calculated to be at -0.7 m, i.e. at the tunnel floor in a radius of $0\text{-}1$ m around the borehole.

The lower limb of reflector 2 can be observed from the borehole intersection at 0.8 m and further away to a distance of 4 m outside the borehole. The reflector indicates either the lithological contact between diorite and red fine-grained granite at 1.25 m, or a pegmatite at $1.35\text{-}1.40$ m. The α -angle of the lithological contact is 39° , and the angle of the pegmatite is 51° . Corresponding angle of the radar reflector is 53° . It is difficult to decide which structure is indicated by the radar reflector, but probably is the correlation with the lithological contact most suitable.

The lower limb of the medium strong reflector 3 is calculated to intersect the borehole at 2.1 m. According to the core log there are three structures possible to be used for the correlation. There is a lithological contact between red fine-grained granite and diorite at 1.8 m, a pegmatite at $2.1\text{-}2.15$ m, and a fracture at 2.25 m. However, interpretation of BIPS-logged structures shows that the α -angle of the lithological contact is 64° , the pegmatite is 32° , and the fracture is 29° . The corresponding angle of the radar reflector is 53° . Best fitness between radar reflector and BIPS-structures is achieved with the lithological contact.

Reflector 4 occurs at 2.7 m. The lower limb of the reflector can be observed from the borehole to a distance of about 2.5 m away from the borehole. The reflector is rather strong and easily detected in the moving-average filtered radar map. The core log contains three structures possible to be used for the correlation. There is a fracture at 2.35 m, a pegmatite vein between $2.40\text{-}2.45$ m, and another pegmatite vein between $2.70\text{-}2.75$ m. Results from the BIPS-interpretation shows that the fracture has an α -angle of 28° , the upper pegmatite has the angle 48° , and the lower pegmatite an angle of 69° . The radar reflector has an angle of 51° and thereby is it difficult to decide which of the pegmatite veins are indicated by the radar reflector. However, the intersection length with borehole of the radar reflector shows best agreement with the lower pegmatite.

The upper limb of the strong reflector 5 intersects the borehole at 3.8 m. The reflector is seen from the intersection with borehole to a distance of 2 m outside the borehole. The core log shows a red fine-grained granite between $3.75\text{-}4.30$ m. Reflector 5 indicates the upper contact. Interpretation of BIPS-logging shows an α -angle of 41° , and the corresponding angle of the radar reflector is 49° .

The lower limb of the strong reflector 6 is interpreted to intersect the borehole at 4.1 m. The limb is visible from the borehole to a distance of about 1.5 m outside the borehole. The reflector occurs at the lower contact of the red fine-grained granite between $3.75\text{-}4.3$ m, mentioned above. The angle to borehole axis of the reflector is 53° and the corresponding angle of the BIPS-interpreted contact is 57° .

Reflector 7 at 6.0 m is easily detected in the moving-average filtered radar map. The upper limb of the reflector can be traced as a straight line from the borehole intersection to a distance of at least 3 m outside the borehole. The angle to borehole axis of the reflector is 51° . The reflector can be correlated either with a pegmatite at 5.65-5.75 m having the α -angle 73° , or with a red fine-grained granite at 6.40-6.50 m having the angle 55° . Best fit is achieved with the granite section.

Reflector 11 at 6.7 m exhibits a small magnitude in the radar map. The upper limb can be observed close to the borehole. The angle to borehole axis is 61° . The core log shows a fracture at 6.65 m and corresponding angle of the fracture interpreted from the BIPS-logging is 69° .

Two reflectors are interpreted to intersect below the end-point of the borehole, these are reflector 8 at 9.5 m and reflector 9 at 10.1 m.

Table 6-9 Reflectors identified from high frequency antenna measurement in borehole KD0092G01.

Reflector ID	Depth of inter-section (m)	Angle of inter-section (degree)	Magnitude 1= weak 2= medium 3= strong U= uncertain A= moving average map	Position of geological structure (m)	Character of geological structure	Angle of inter-section of BIPS-structure (degree)	Orientation of BIPS-mapped structure
10	-0.7	40-50	2A	At floor in a radius of 0-1 m around the borehole			
1	0.1	90	3		Floor		
2	0.8	53	2A	1.25	Contact diorite/ red fine-grained granite	39	51/013
3	2.1	53	2A	1.35-1.40	Pegmatite	51	39/014
				1.8	Contact red fine-grained granite/ diorite	64	26/354
4	2.7	51	2A	2.1-2.15	Pegmatite	32	58/293
				2.25	Fracture	29	61/256
				2.35	Fracture	28	62/232
				2.40-2.45	Pegmatite	48	42/308
5	3.8	49	3A	2.70-2.75	Pegmatite	69	21/035
				3.75-4.3	Red fine-grained granite	41	49/353
6	4.1	53	3A	3.75-4.3	Red fine-grained granite	57	33/342
7	6.0	51	2A	5.65-5.75	Pegmatite	73	17/262
				6.40-6.50	Red fine-grained granite	55	35/027
11	6.7	61	1A	6.65	Fracture	69	21/129
8	9.5	45	2A		Below		
9	10.1	44	2A		Below		

7 Conclusions

The result from the 250 MHz radar measurement in the nine boreholes is considered good. The strongest reflectors are generally those representing the tunnel floor and the tunnel roof. Reflectors representing geological features are generally weak or medium strong. Moving-average filtered radar maps were used in order to enhance those reflectors. The resolution of the radar maps is good and even single fractures have been identified in the radar maps.

A total of 102 reflectors have been interpreted from the 250 MHz antenna measurement in the boreholes. If reflectors from tunnel floor, borehole bottom, and reflectors intersecting above or below the borehole are excluded, then the remaining number of reflectors intersecting the borehole will be 60. Of the 60 radar reflectors were 57 able to be correlated with geological structures mapped in the core logs. Consequently there was no explanation in the core logs for 3 of the radar reflectors.

For the correlation between 250 MHz radar reflectors and BIPS-interpreted structures was a number of 60 radar reflectors used. Of those 60 radar reflectors have 54 been correlated with BIPS-structures in the boreholes. The agreement between α -angles for radar reflectors and BIPS-structures was considered very good. Of the radar reflectors have 40 been correlated with good result, i.e. with a difference in α -angle less than 20° . Uncertain result was achieved for the correlation of 9 radar reflectors with BIPS-interpreted structures, i.e. the difference was between 20 - 35° . Finally, for 5 radar reflectors the difference in α -angle was large, i.e. more than 35° . BIPS-data was not available for 2 radar reflectors since they were interpreted to intersect the borehole below the end of the BIPS-logging. Consequently there was no suitable BIPS-structure for 4 of the radar reflectors.

References

Carlsten S, 1998. Borehole radar measurements in KA3573A, KA3600F, and G-boreholes. Äspö HRL Progress Report HRL-98-16. SKB, Stockholm, Sweden.

Carlsten S, 1996. Results from borehole radar measurement in KA2563A. Äspö HRL Technical Note TN-96-20b. SKB, Stockholm, Sweden.

Sandberg E, Olsson O, Falk L, 1991. Combined interpretation of fracture zones in crystalline rock using single-hole, crosshole tomography and directional borehole-radar data. *The Log Analyst*, 32(2), 108-119.

Appendix: Bandpass filtered radar maps, moving-average filtered radar maps, and interpretation maps from the 250 MHz measurements.

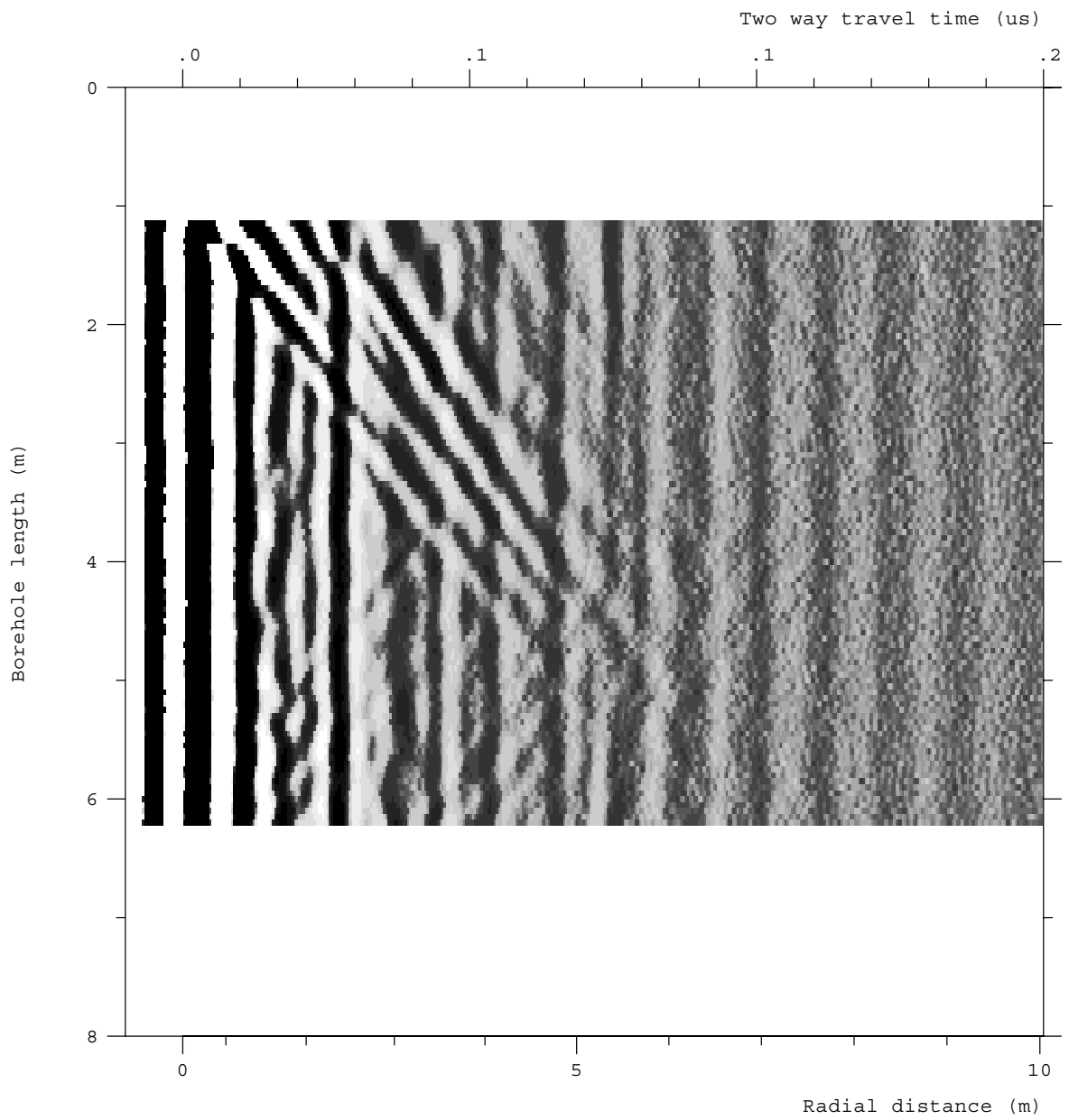


Figure A1 *High frequency radar reflection map for borehole KA3147G001. DC-filtered and bandpass filtered map.*

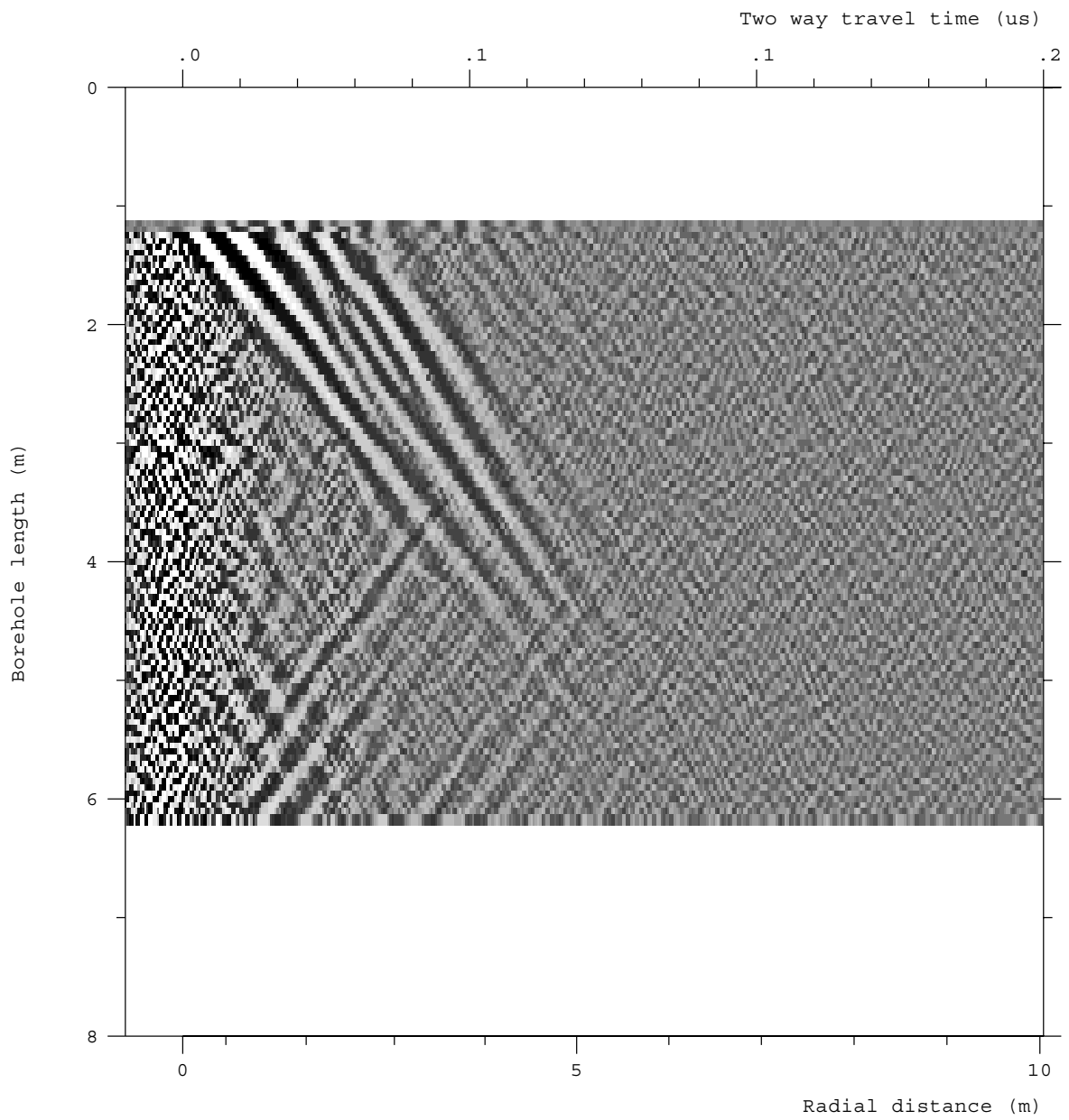


Figure A2 *High frequency radar reflection map for borehole KA3147G001. Moving-average filtered map.*

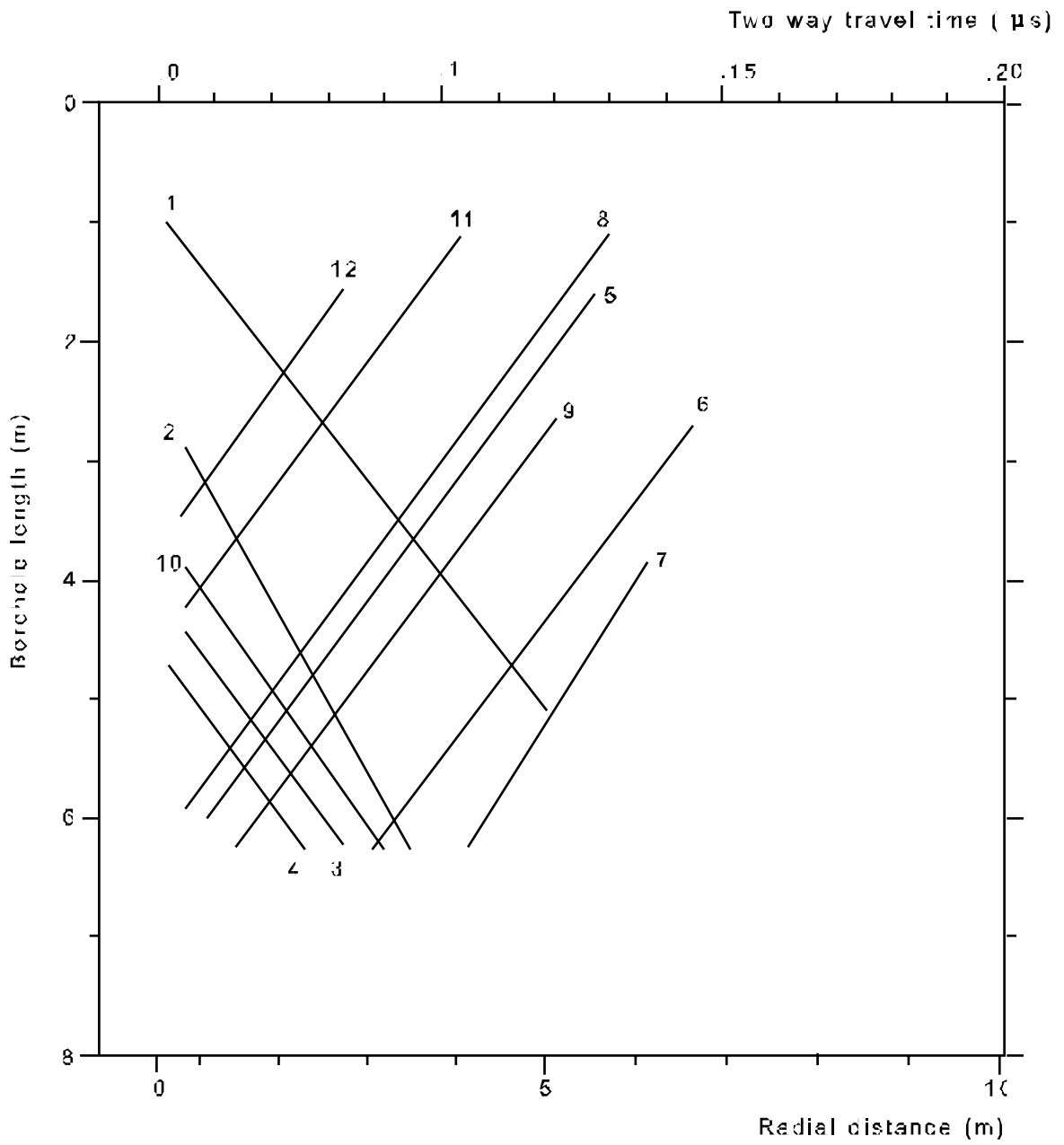


Figure A3 Interpretation map for borehole KA3147G001.

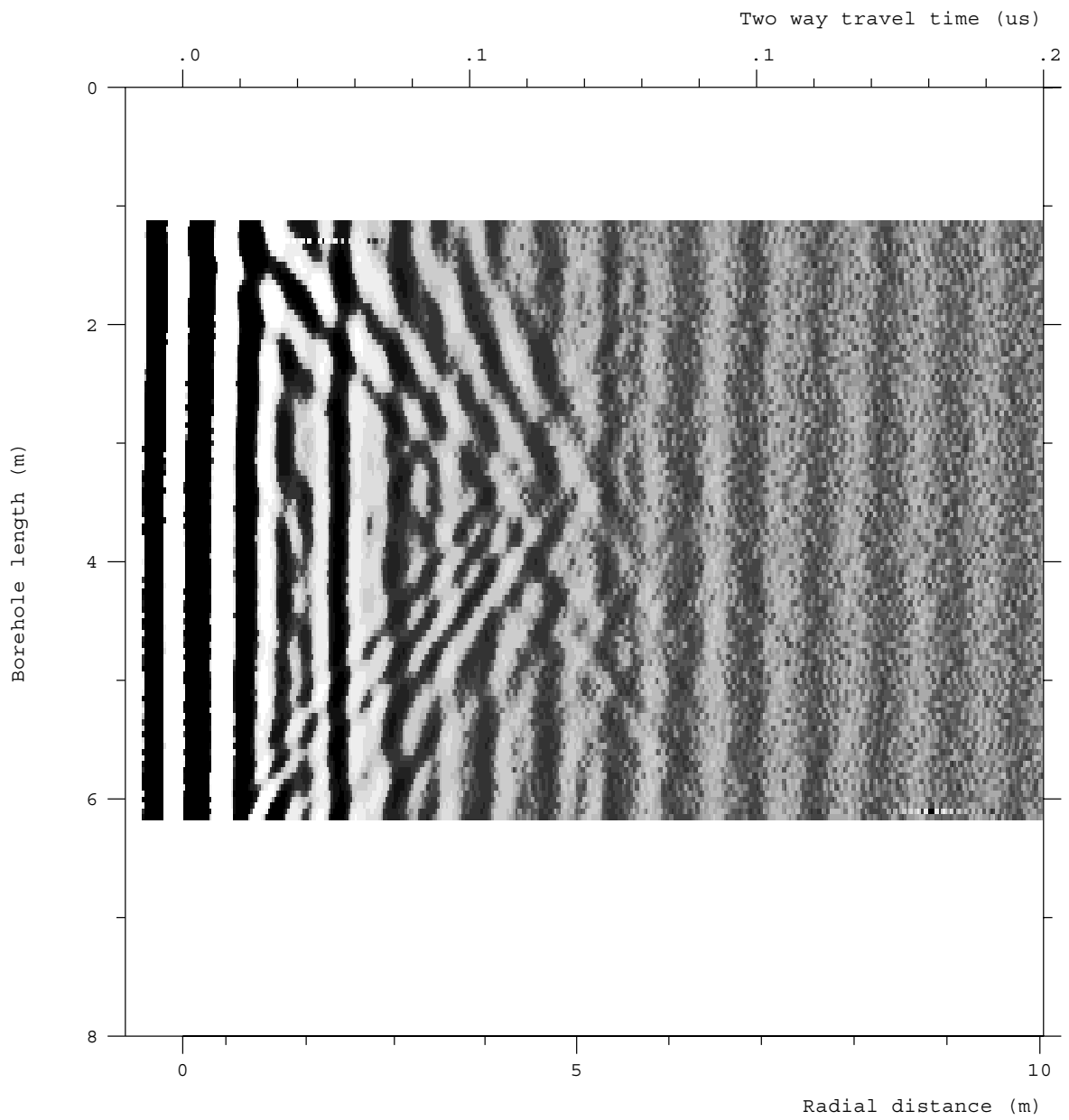


Figure A4 *High frequency radar reflection map for borehole KA3153G001. DC-filtered and bandpass filtered map.*

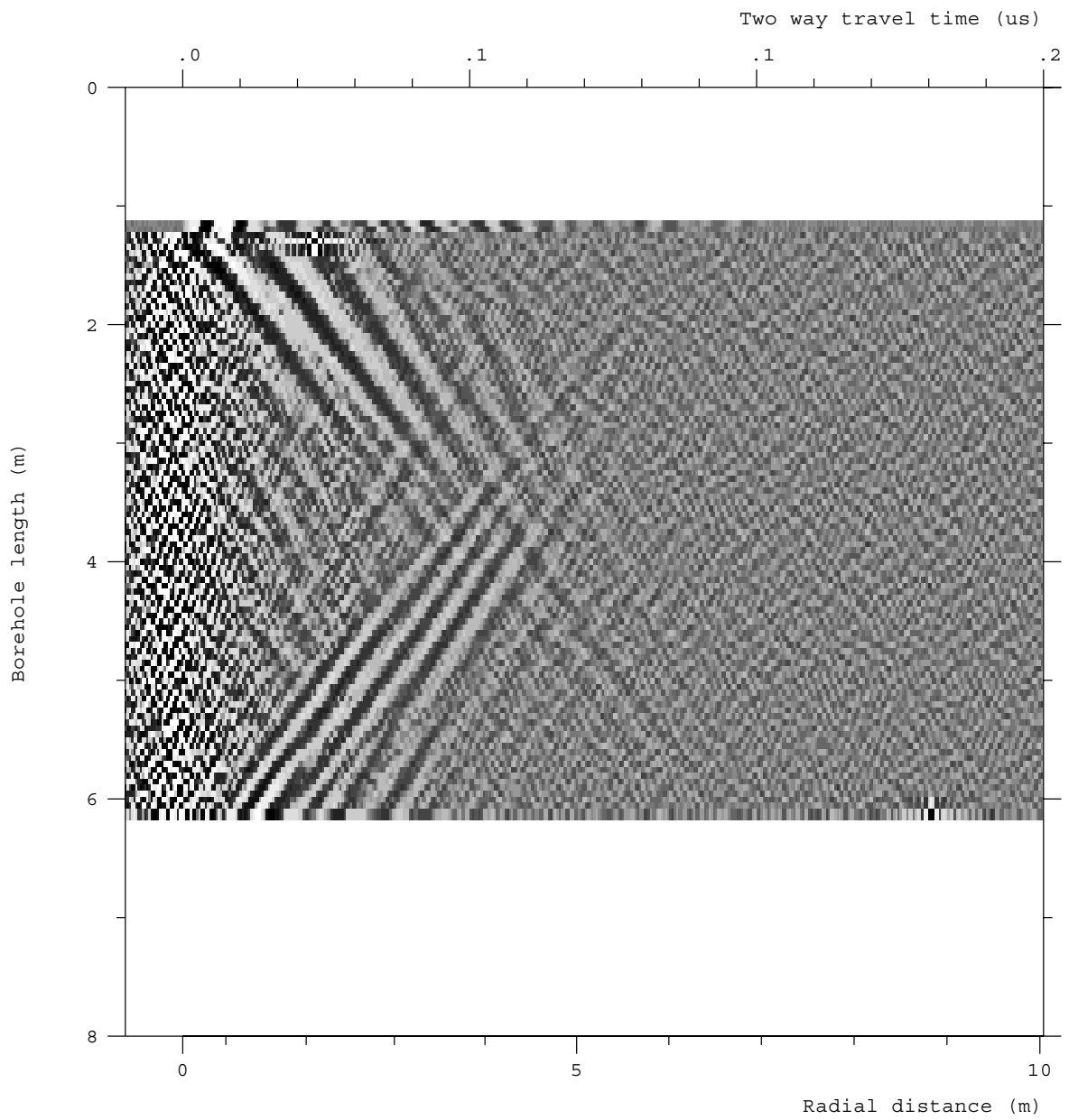


Figure A5 *High frequency radar reflection map for borehole KA3153G001. Moving-average filtered map.*

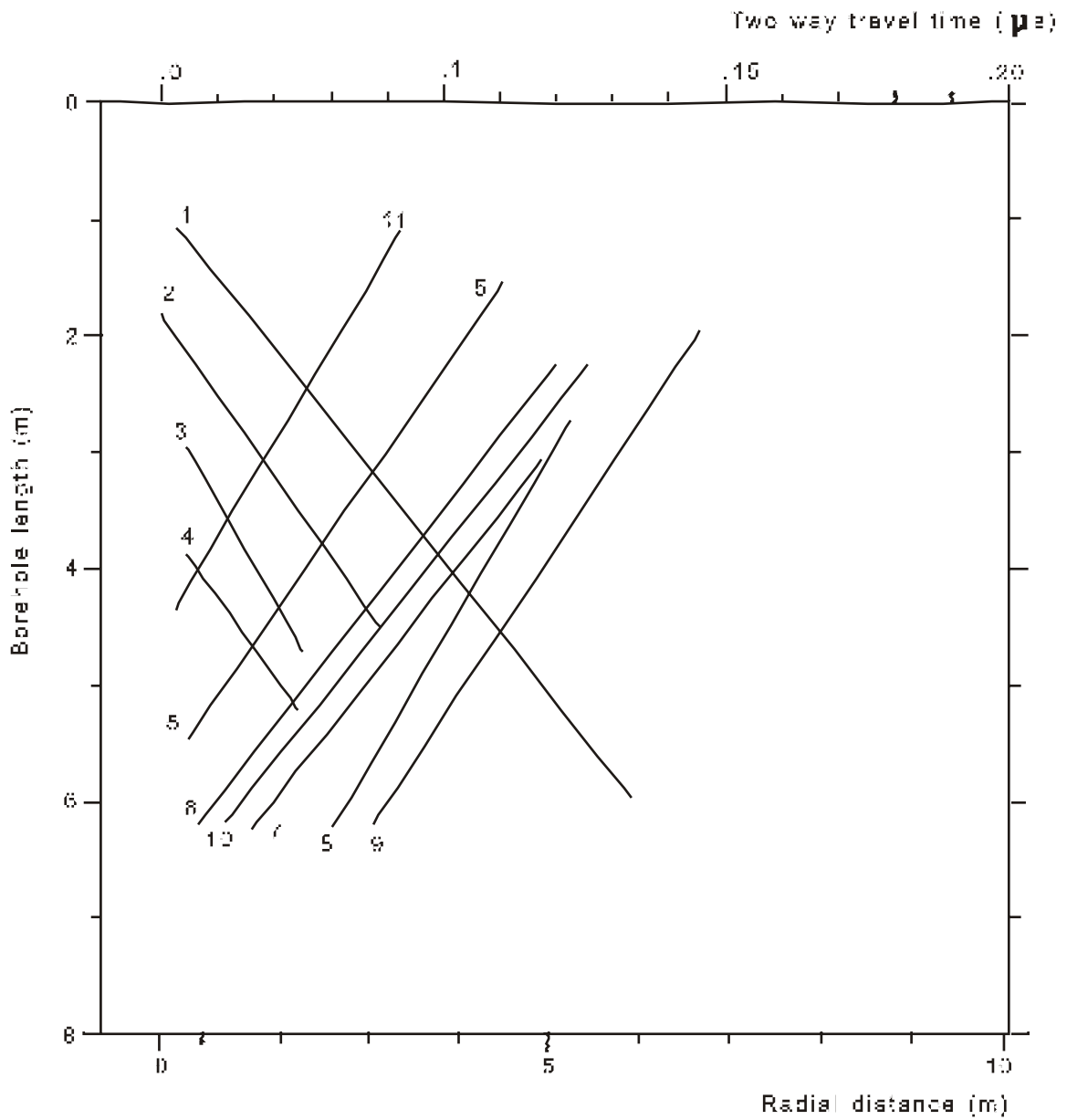


Figure A6 Interpretation map for borehole KA3153G001.

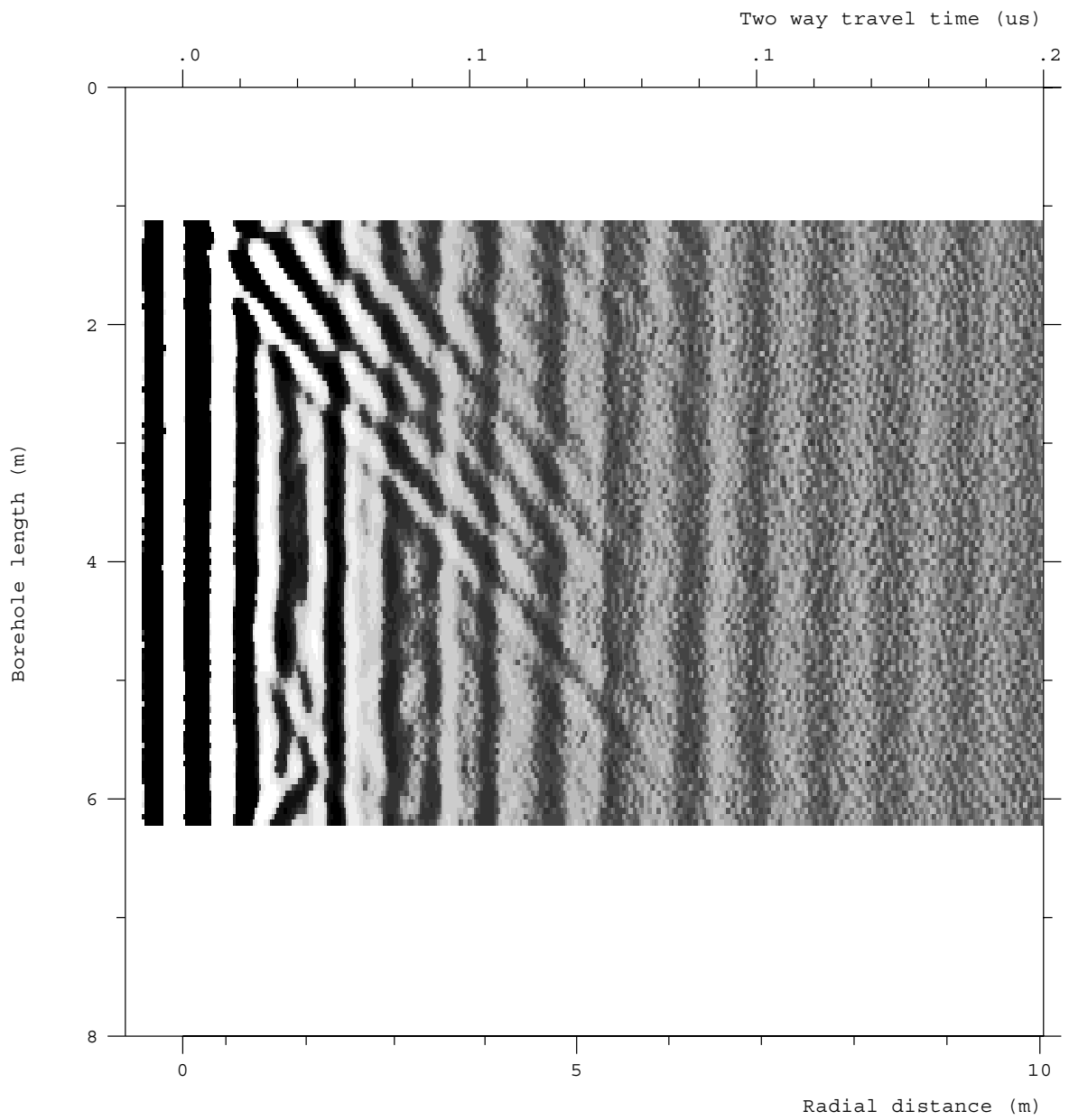


Figure A7 High frequency radar reflection map for borehole KK0025G001. DC-filtered and bandpass filtered map.

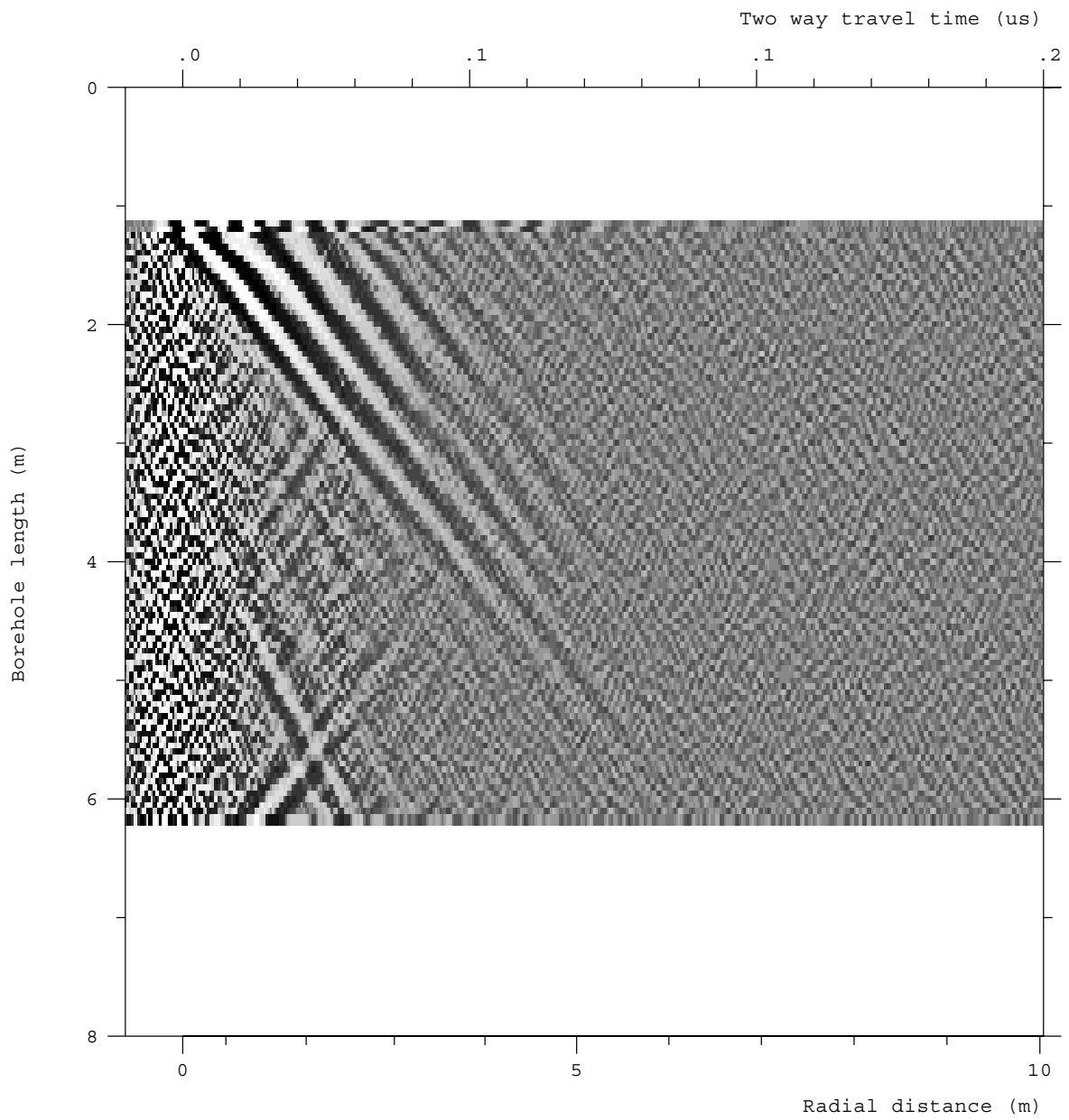


Figure A8 *High frequency radar reflection map for borehole KK0025G001. Moving-average filtered map.*

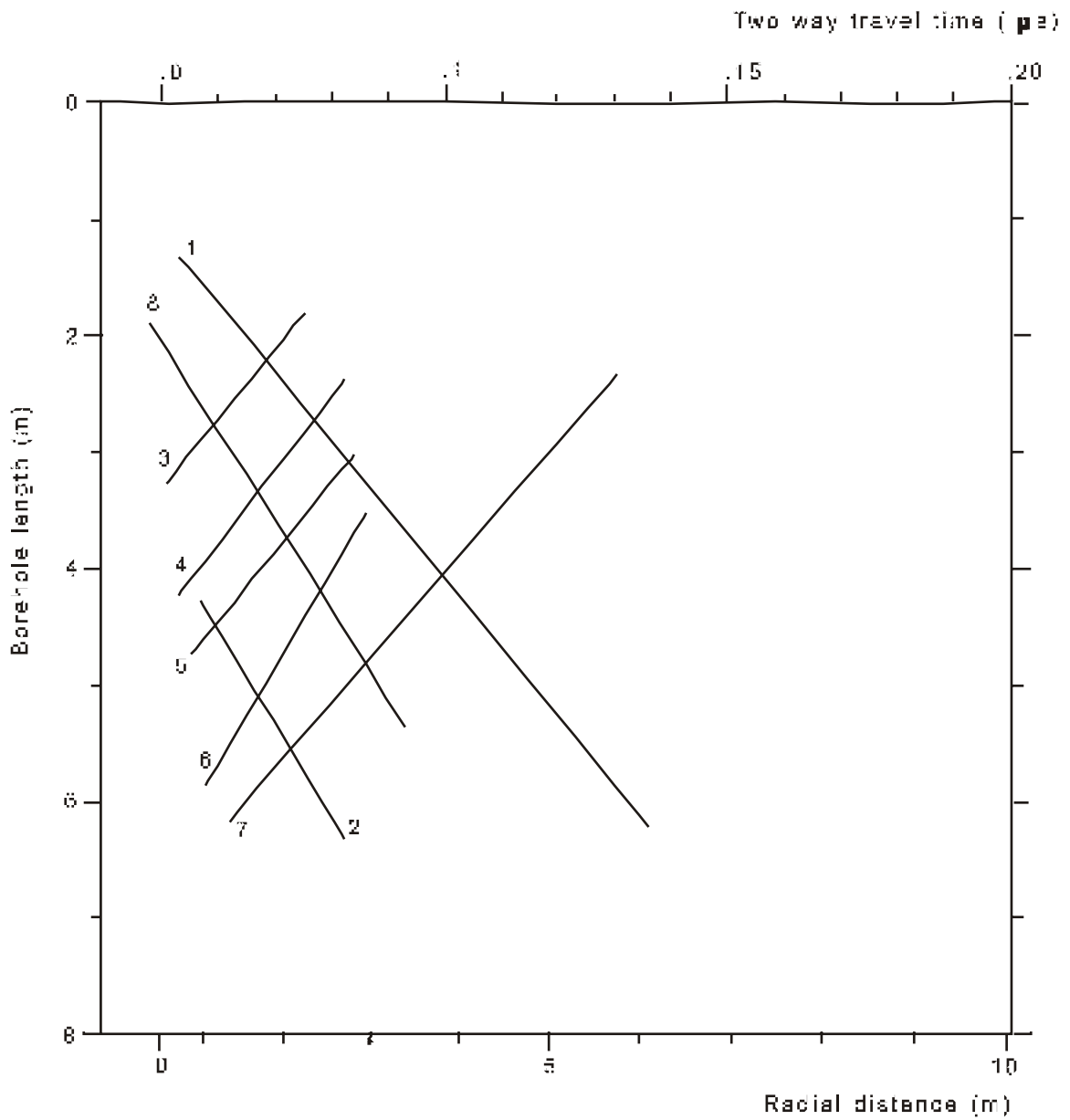


Figure A9 Interpretation map for borehole KK0025G001.

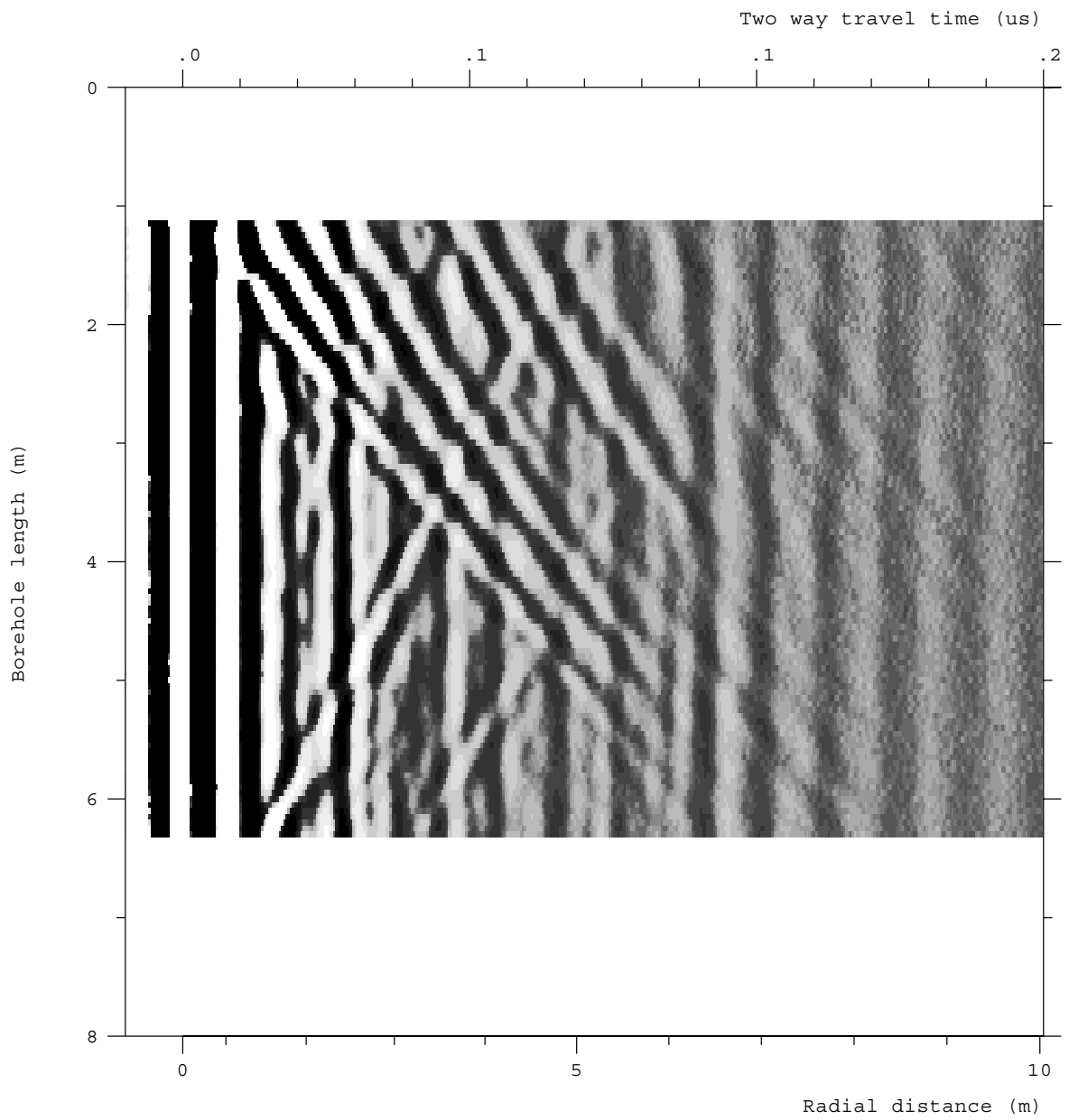


Figure A10 High frequency radar reflection map for borehole KK0031G001. DC-filtered and bandpass filtered map.

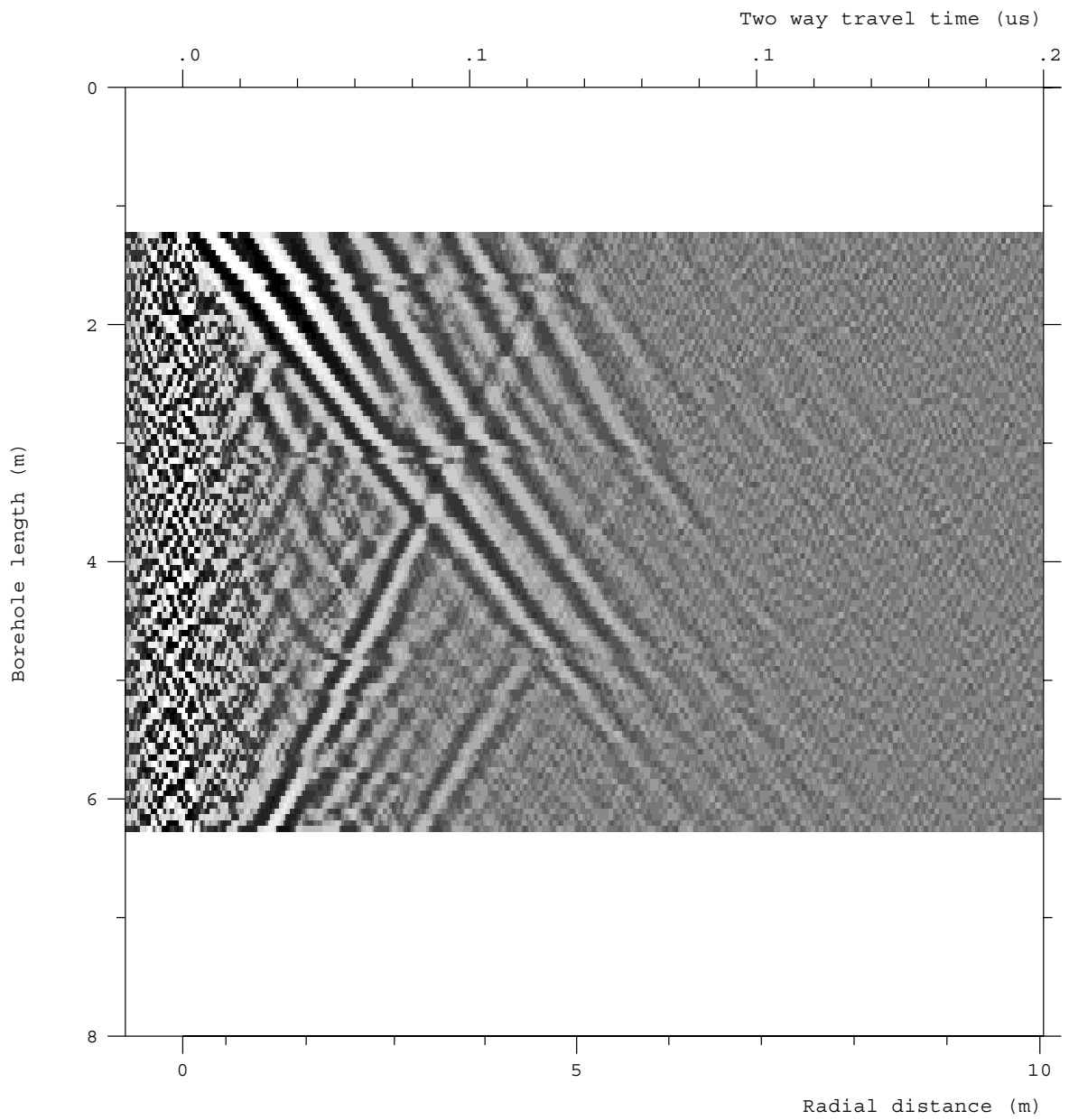


Figure A11 High frequency radar reflection map for borehole KK0031G001. Moving-average filtered map.

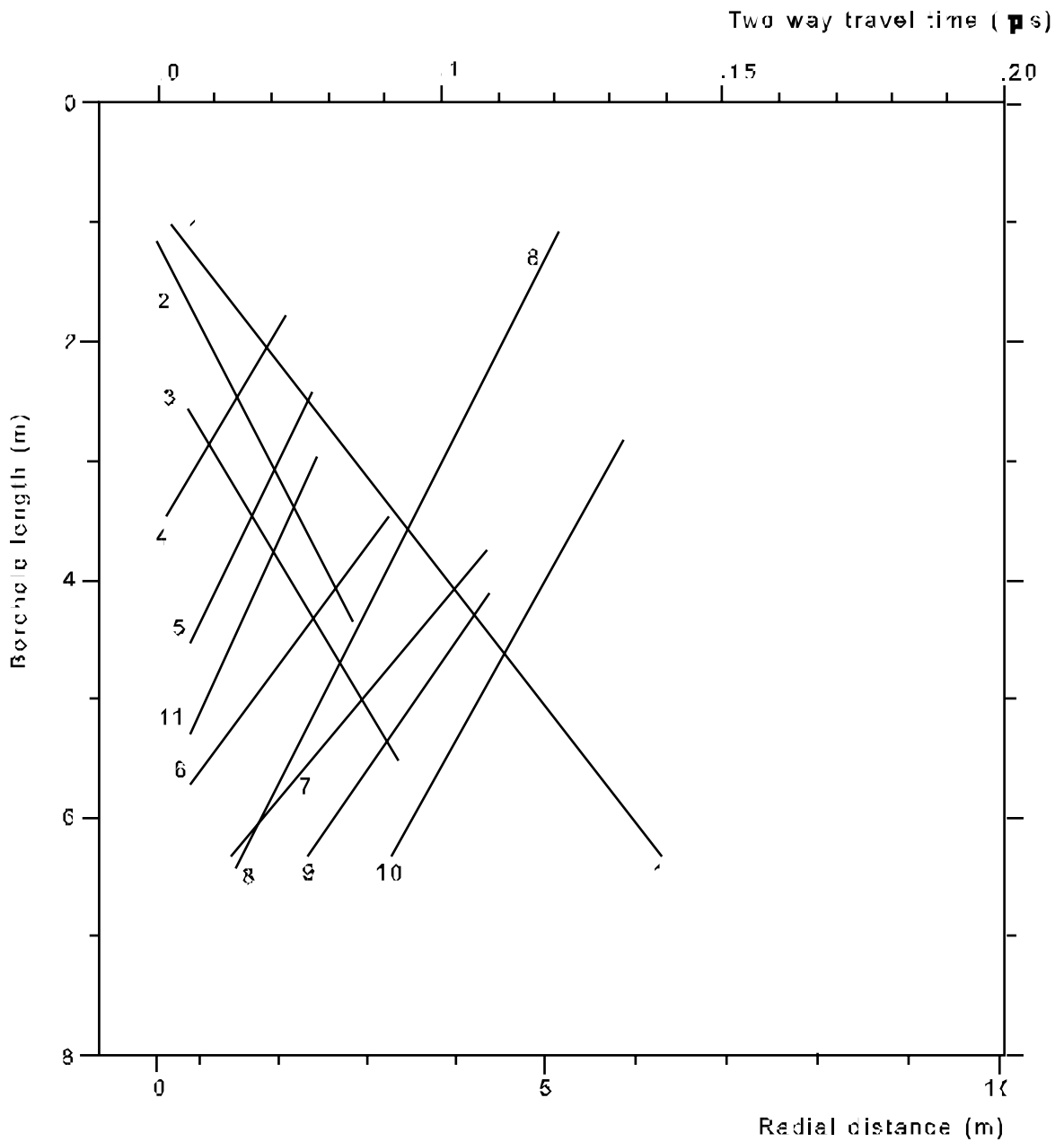


Figure A12 Interpretation map for borehole KK0031G001.

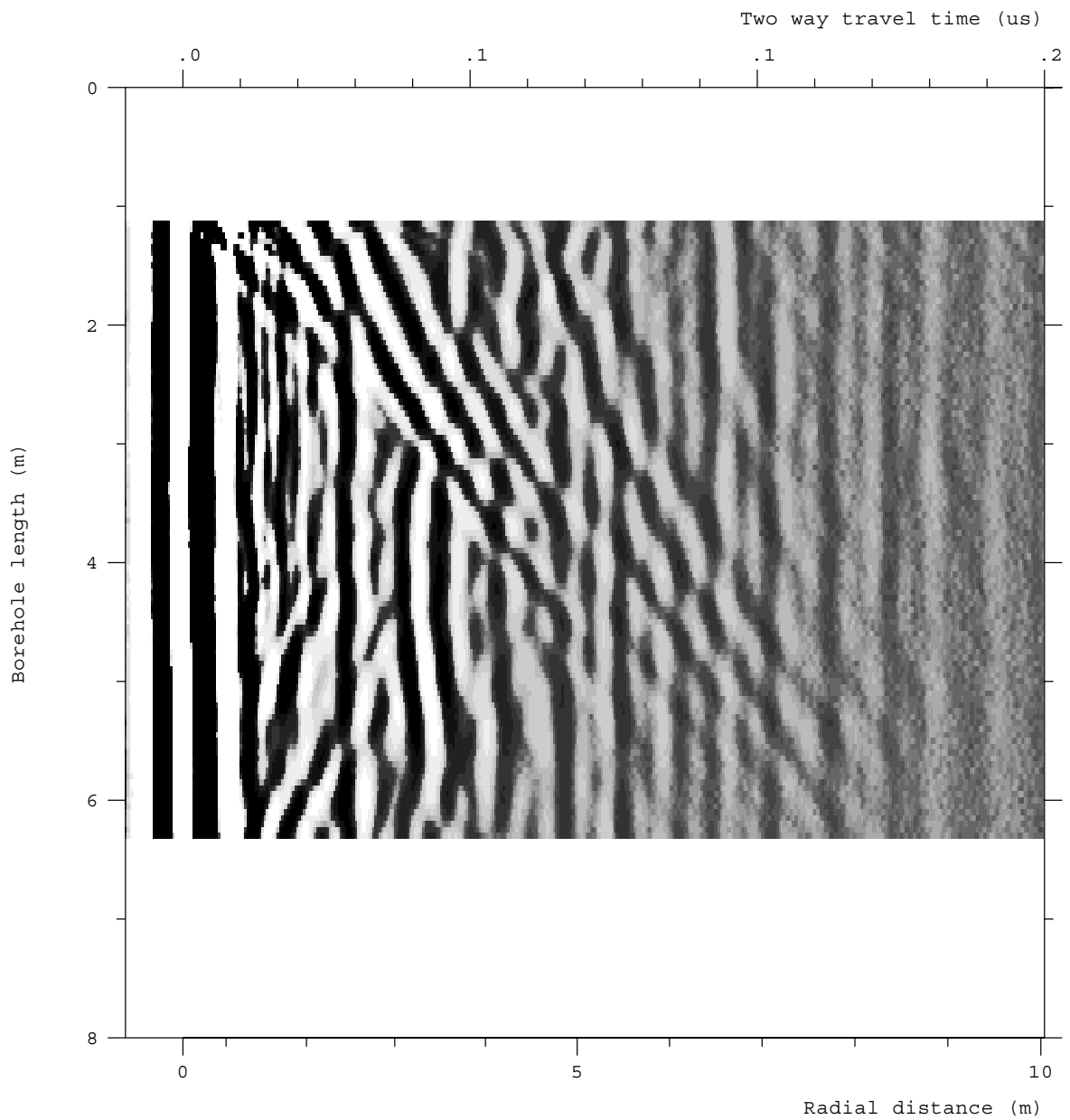


Figure A13 High frequency radar reflection map for borehole KK0037G001. DC-filtered and bandpass filtered map.

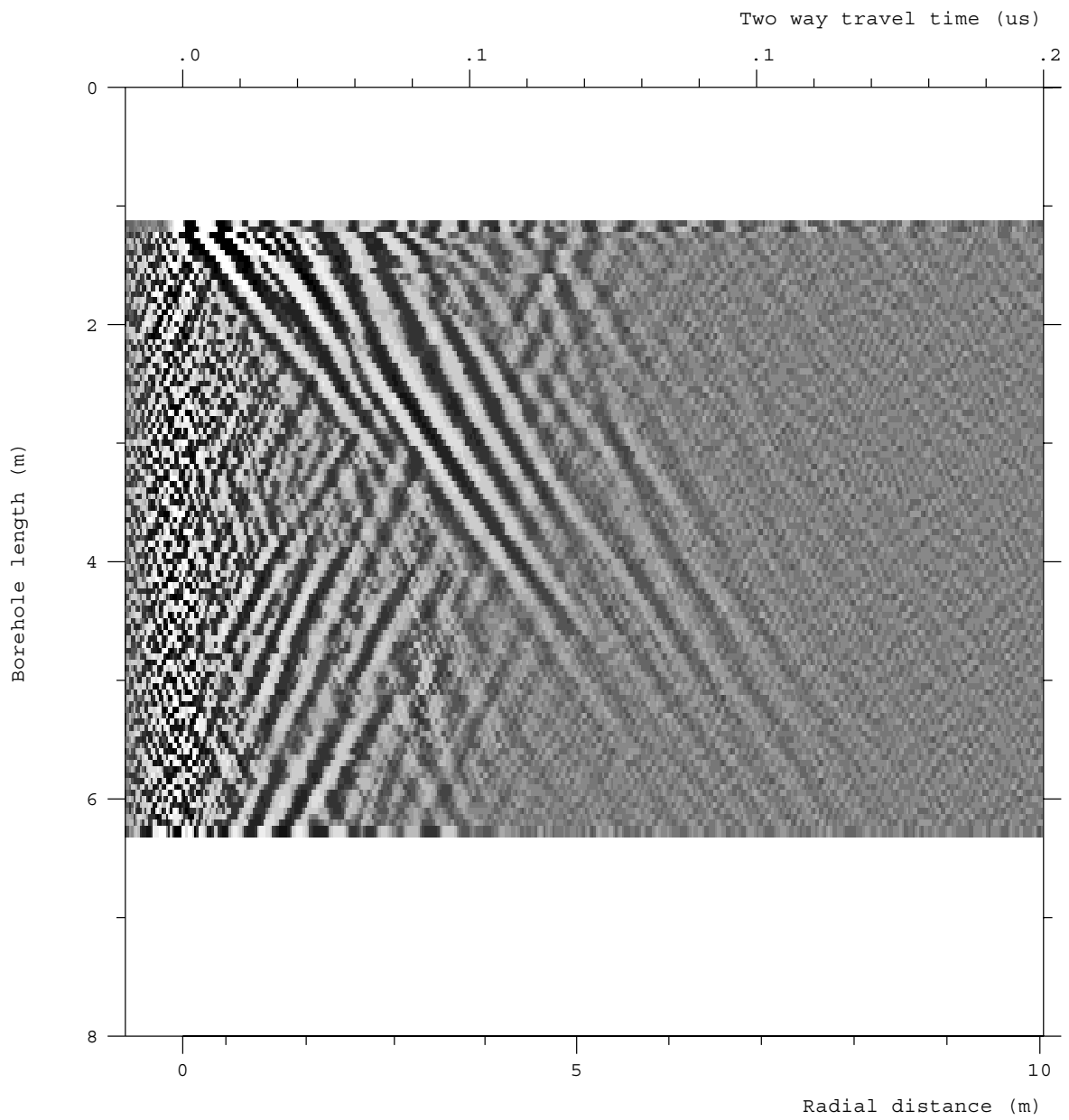


Figure A14 High frequency radar reflection map for borehole KK0037G001. Moving-average filtered map.

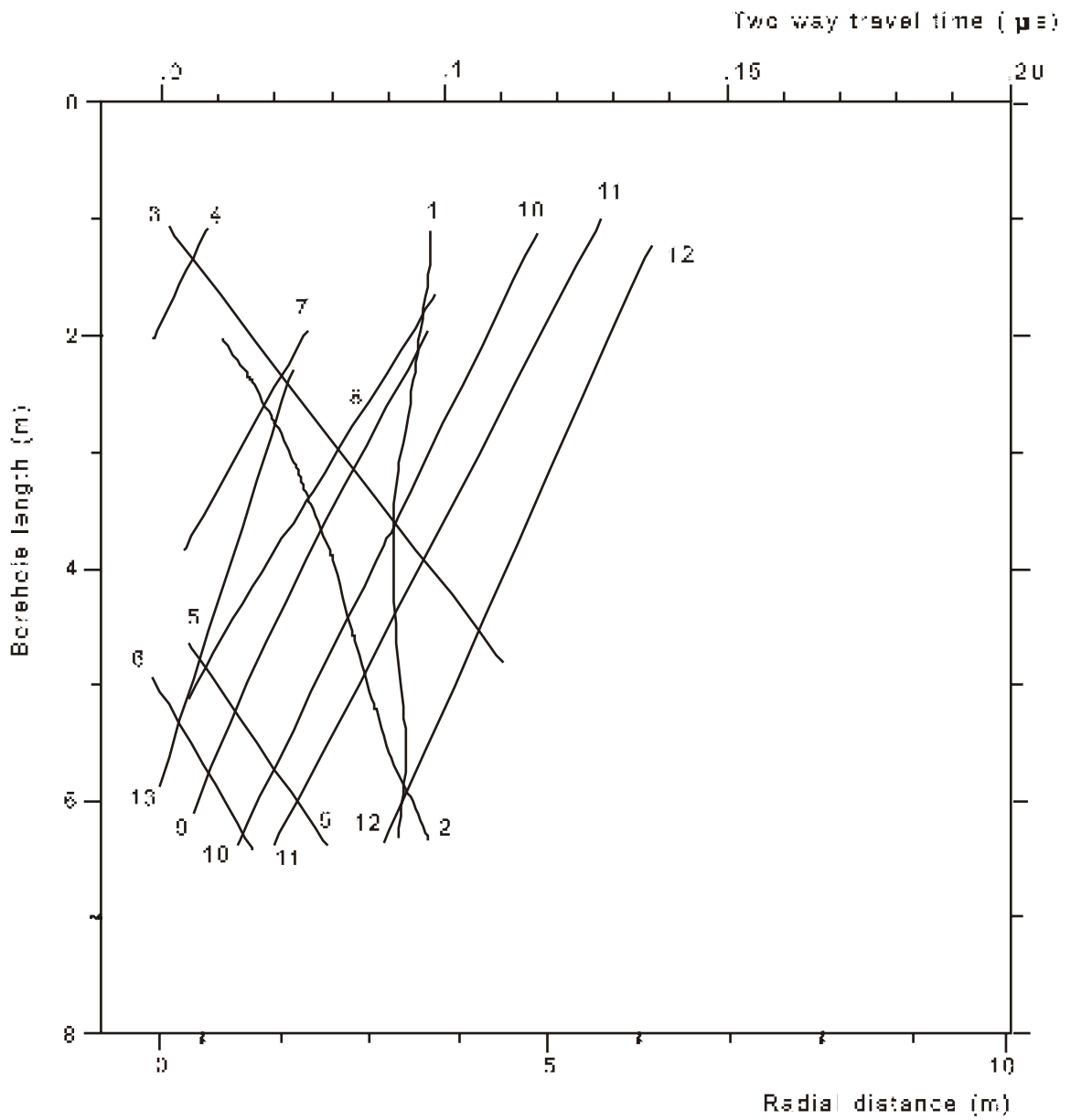


Figure A15 Interpretation map for borehole KK0037G001.

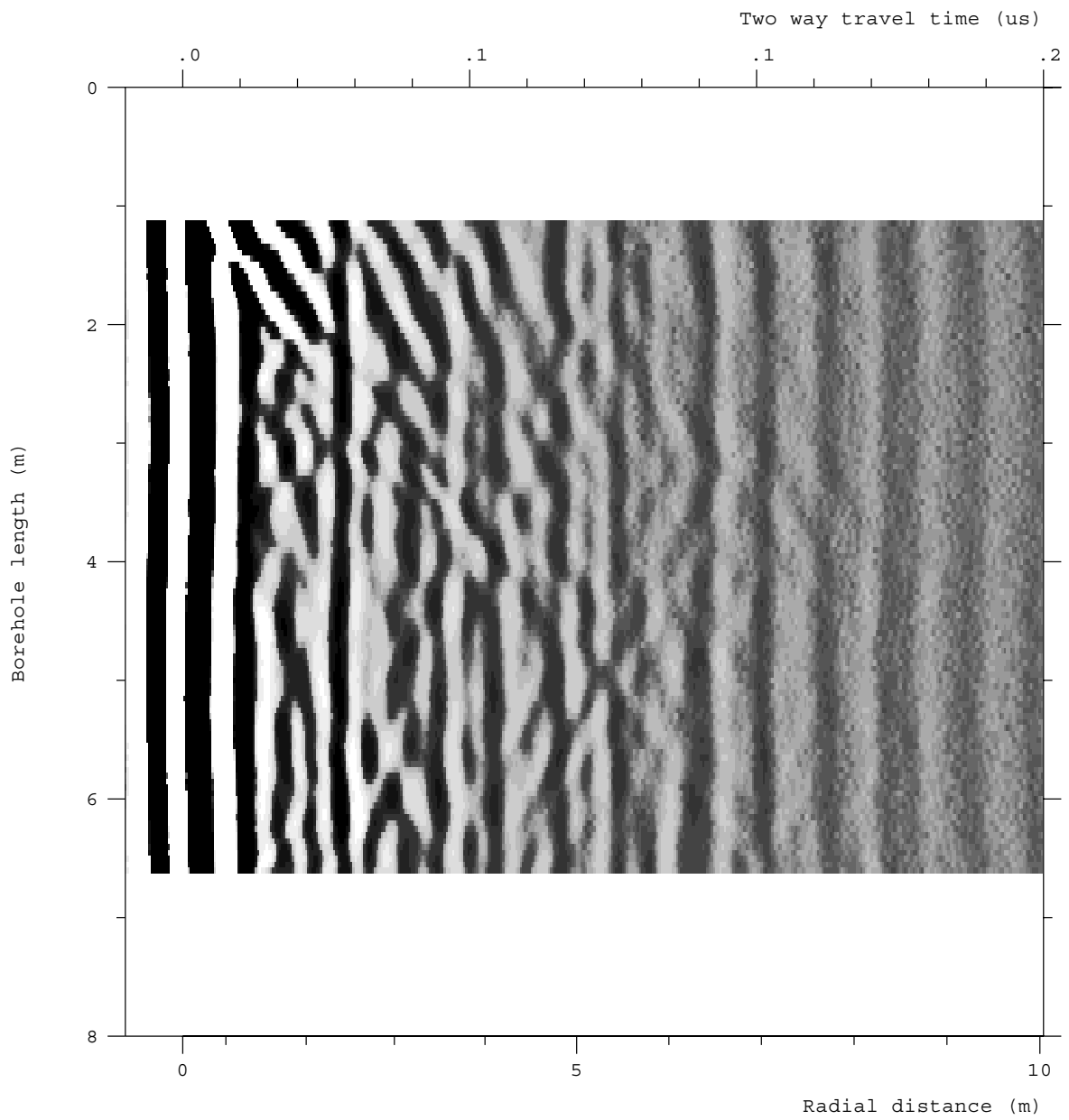


Figure A16 High frequency radar reflection map for borehole KK0045G001. DC-filtered and bandpass filtered map.

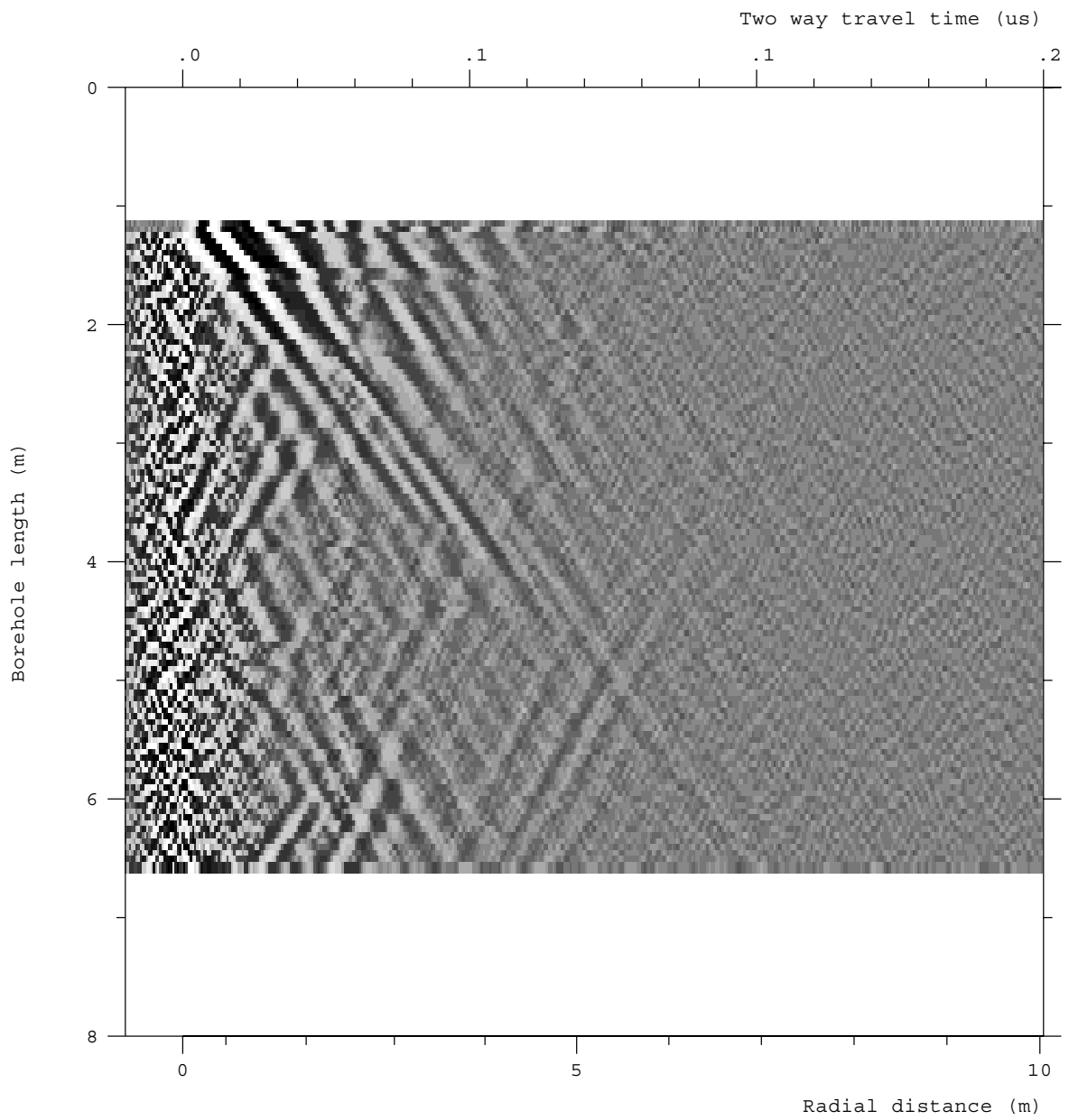


Figure A17 High frequency radar reflection map for borehole KK0045G001. Moving-average filtered map.

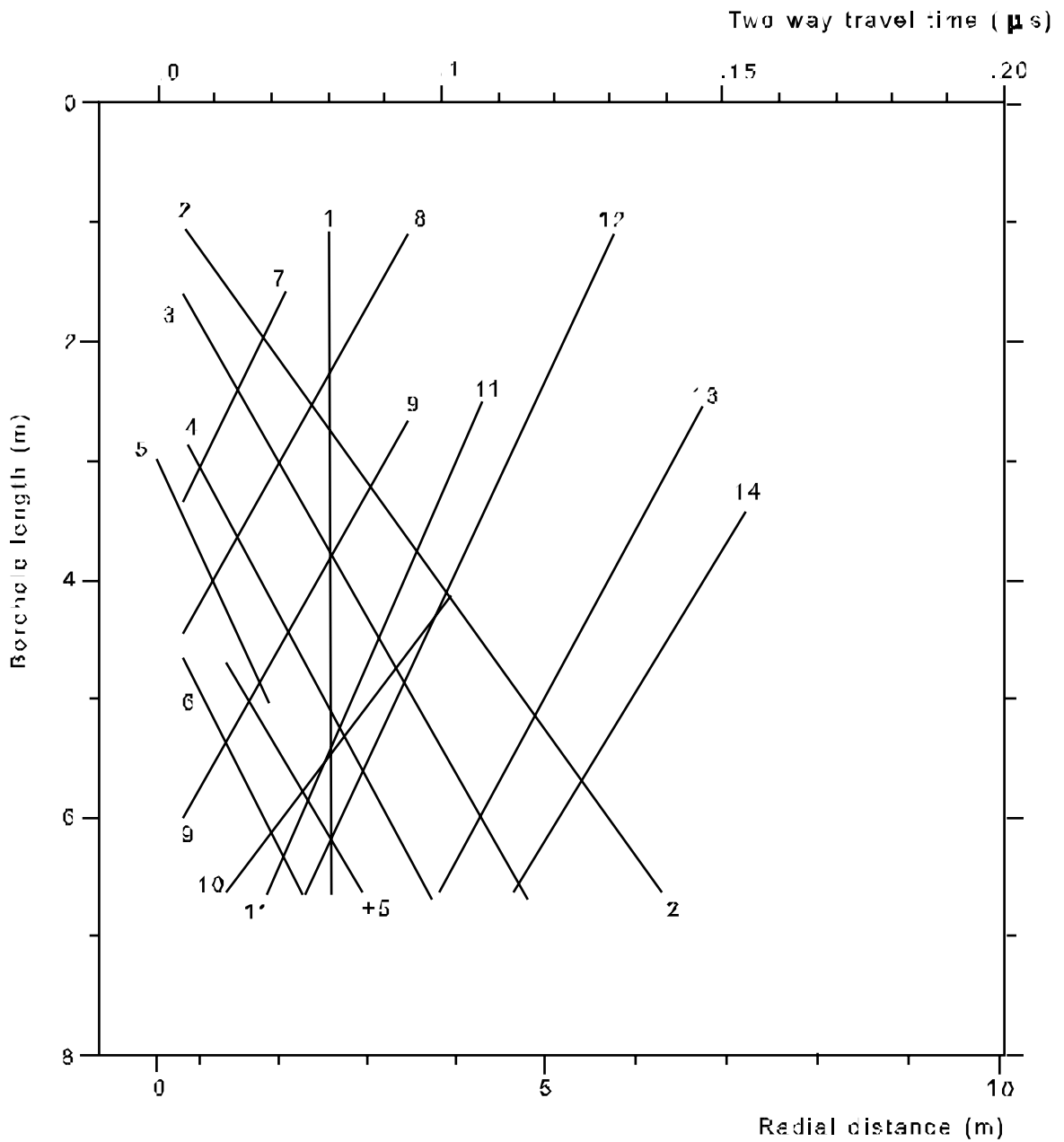


Figure A18 Interpretation map for borehole KK0045G001.

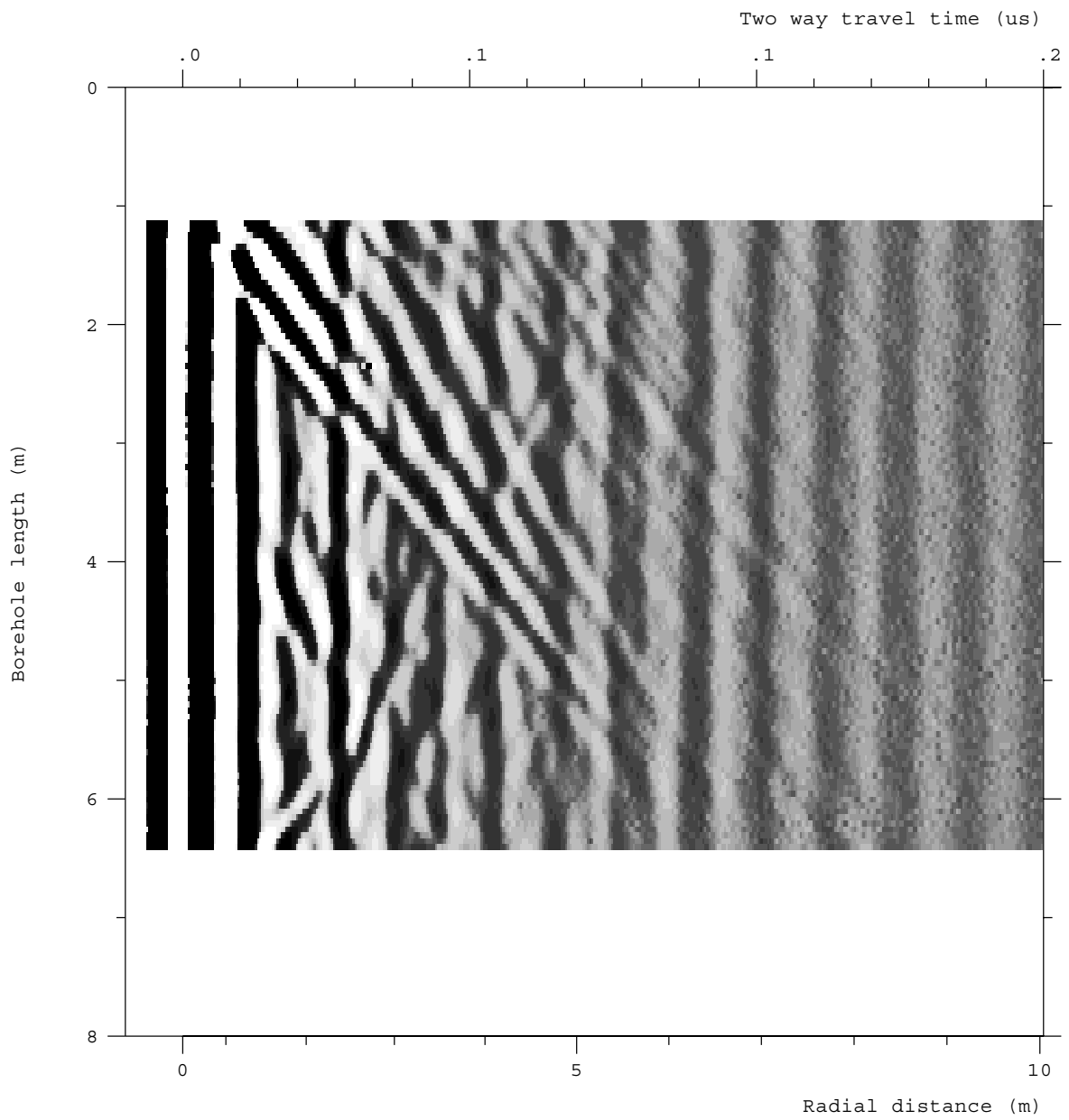


Figure A19 High frequency radar reflection map for borehole KK051G001. DC-filtered and bandpass filtered map.

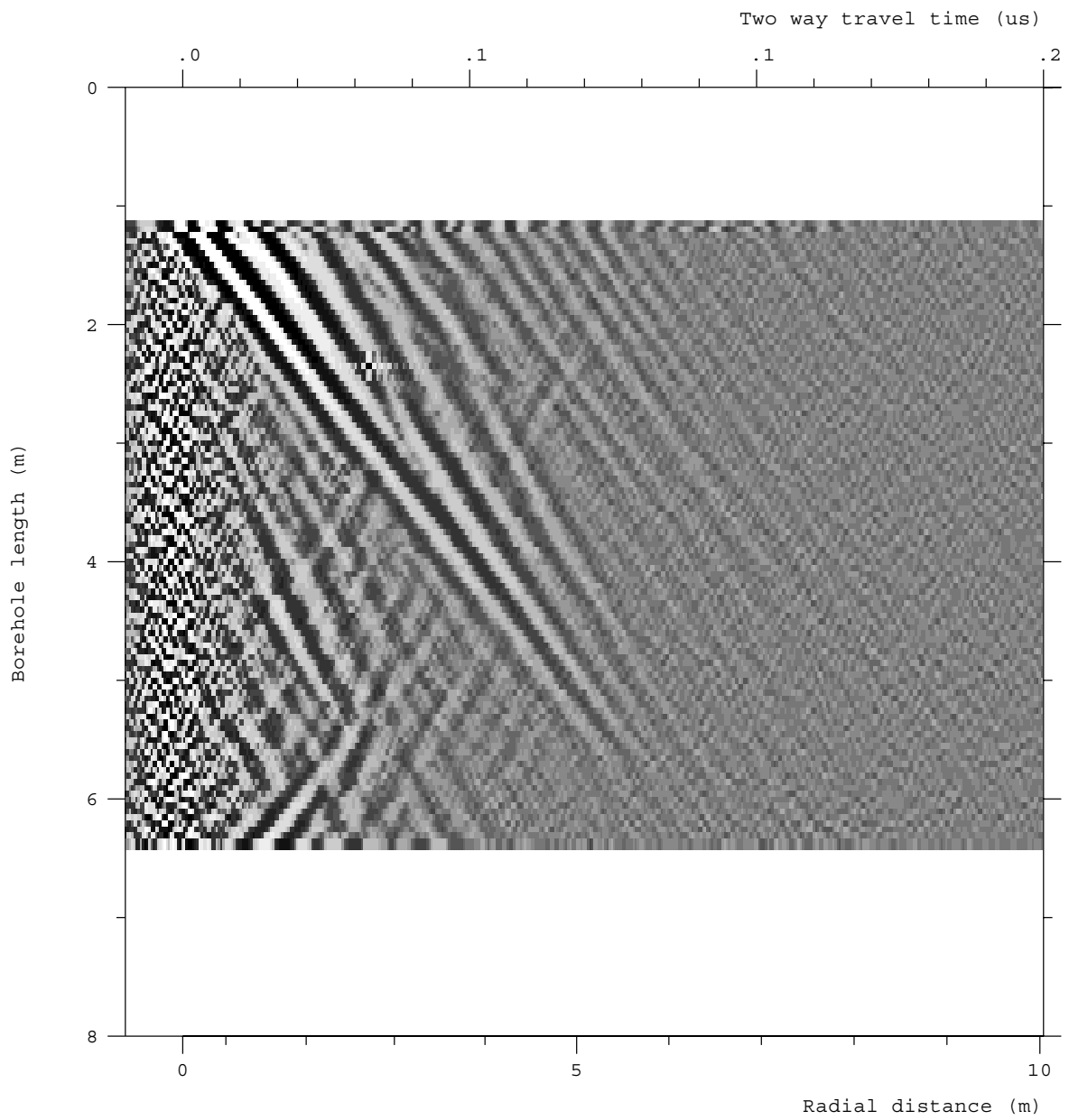


Figure A20 High frequency radar reflection map for borehole KK0051G001. Moving-average filtered map.

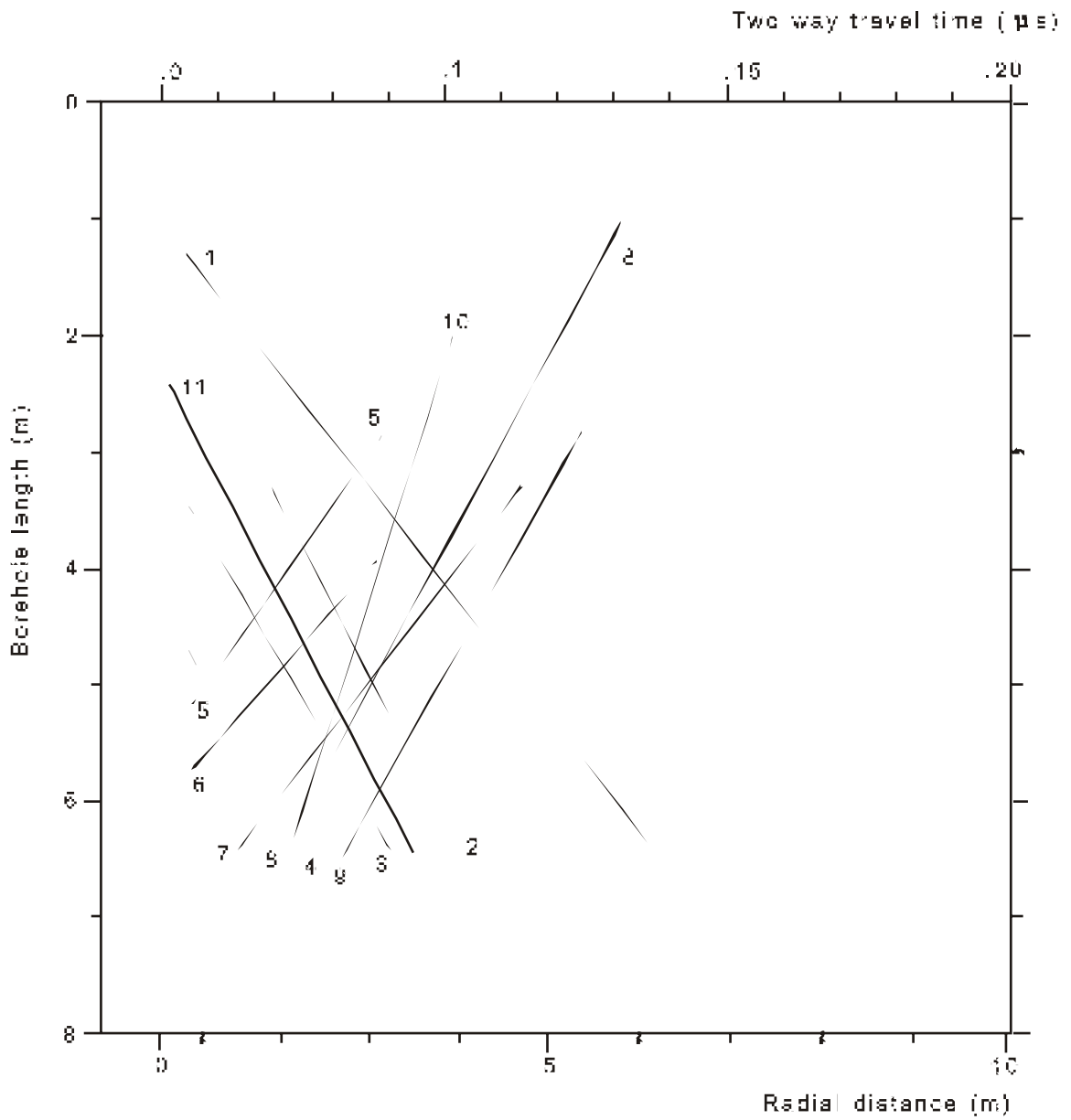


Figure A21 Interpretation map for borehole KK0051G001.

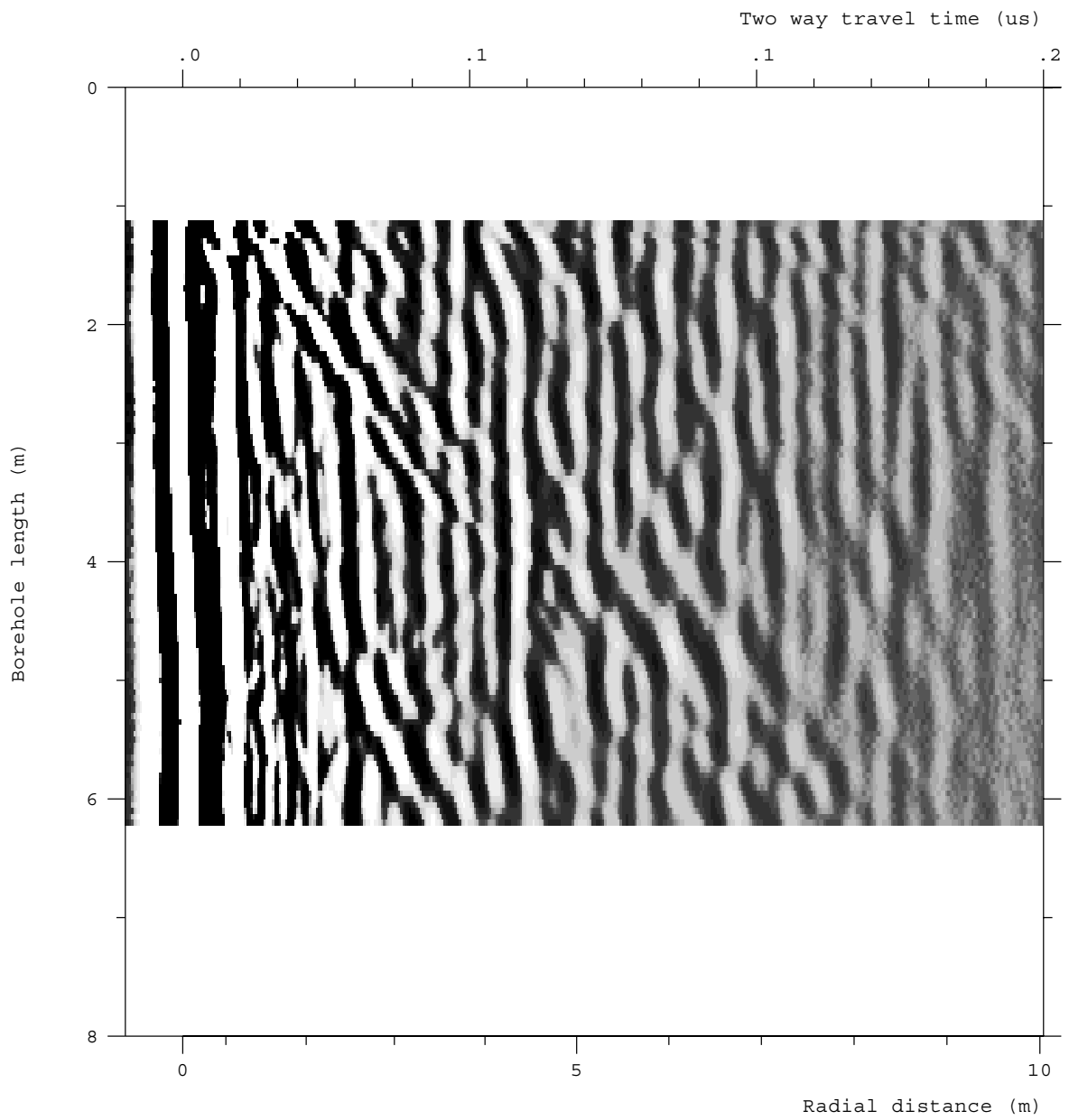


Figure A22 High frequency radar reflection map for borehole KD0086G001. DC-filtered and bandpass filtered map.

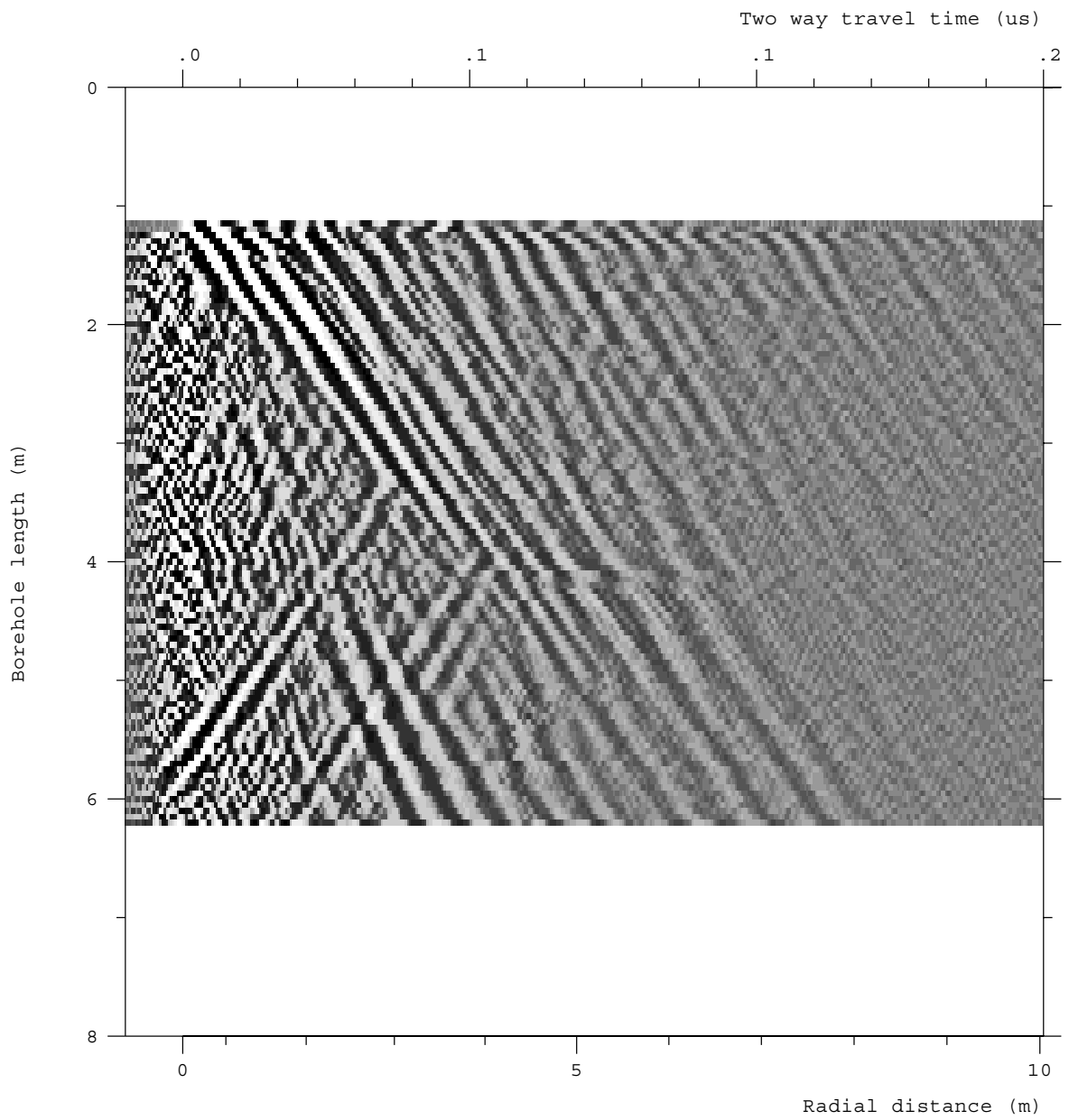


Figure A23 High frequency radar reflection map for borehole KD0086G001. Moving-average filtered map.

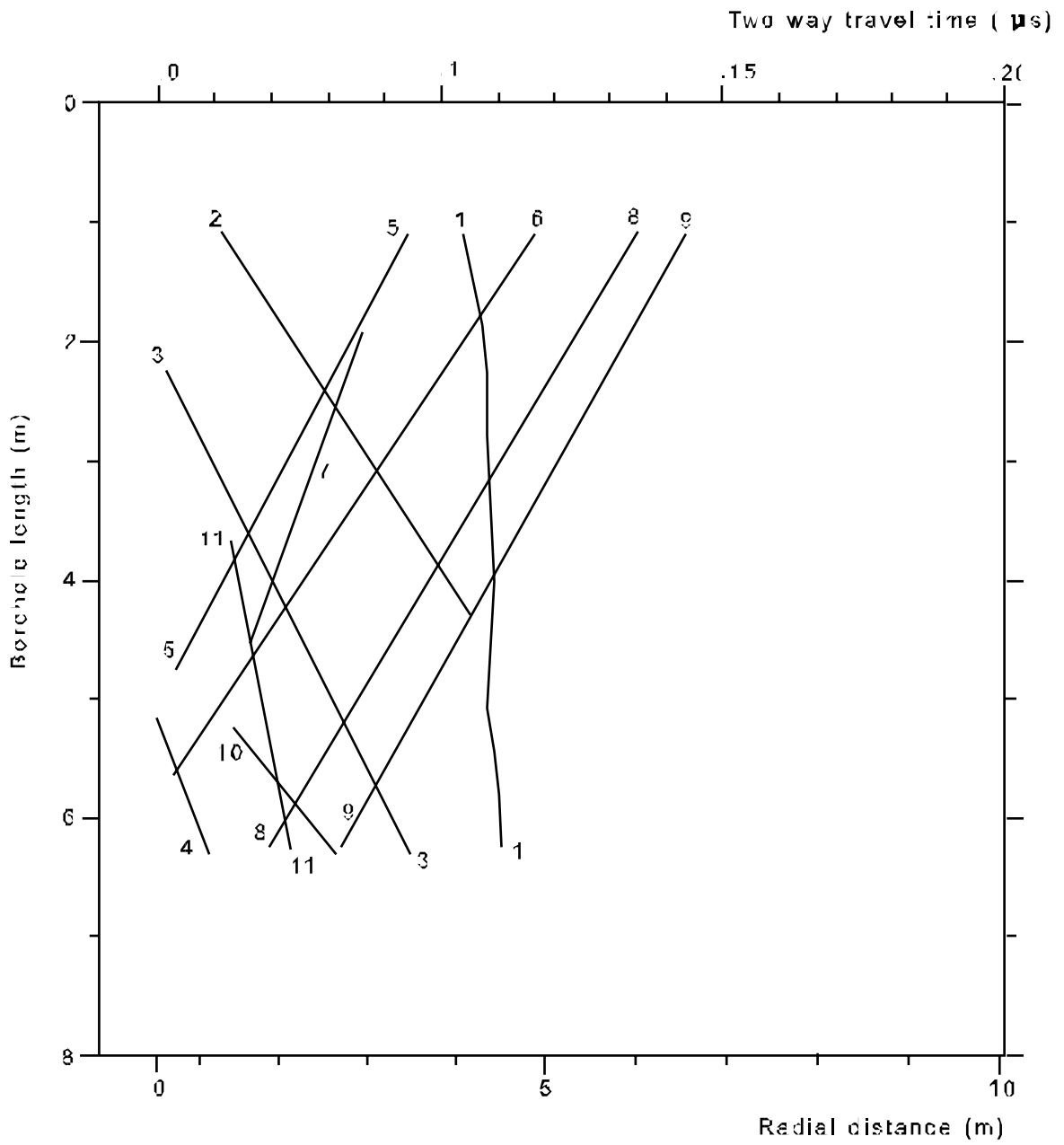


Figure A24 Interpretation map for borehole KD0086G001.

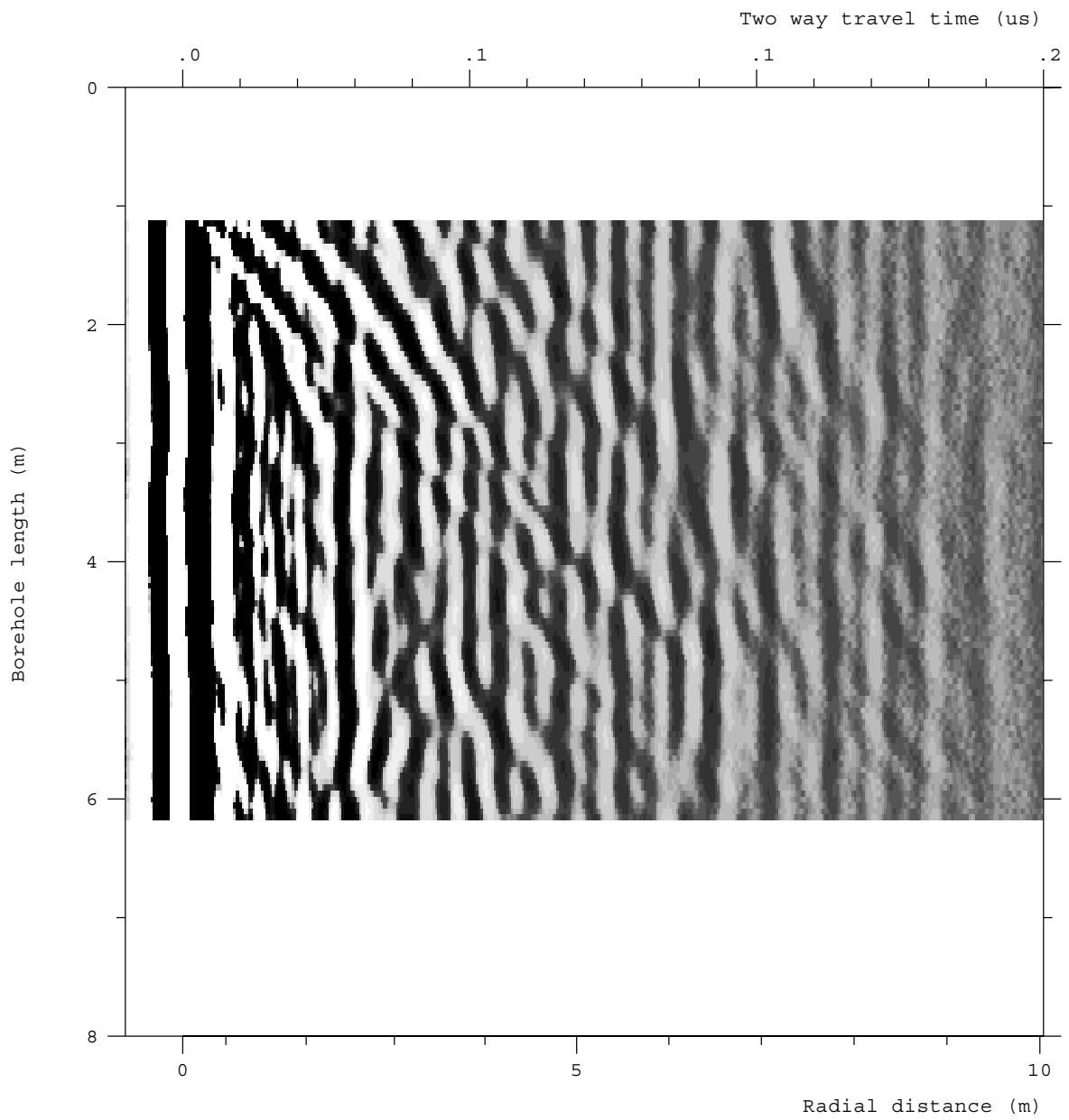


Figure A25 High frequency radar reflection map for borehole KD0092G001. DC-filtered and bandpass filtered map.

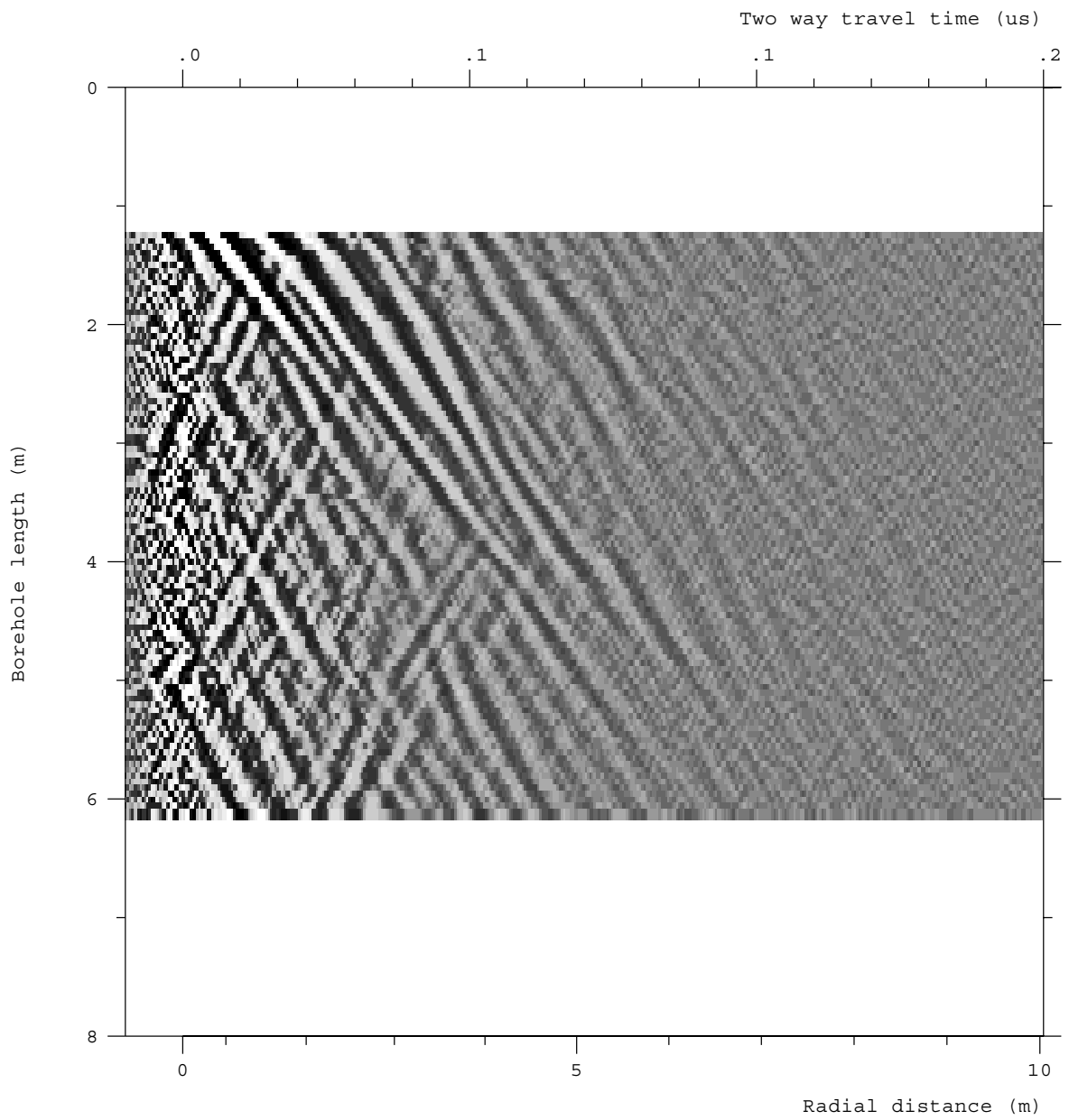


Figure A26 High frequency radar reflection map for borehole KD0092G001. Moving-average filtered map.

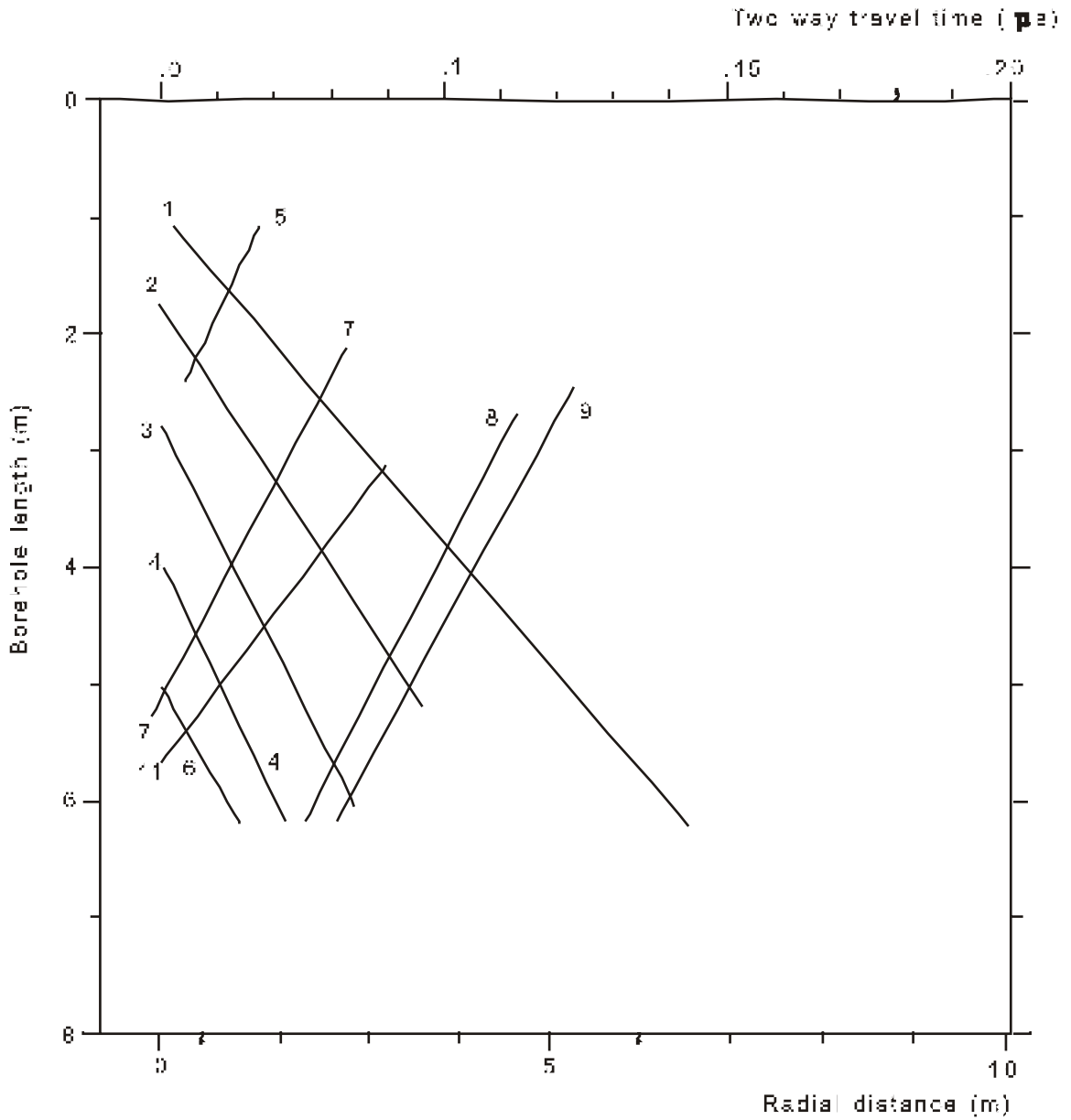


Figure A27 Interpretation map for borehole KD0092G001.